

Supporting Information

Triblock Polyester Thermoplastic Elastomers with Semi-aromatic Polymer End Blocks by Ring-Opening Copolymerization

Georgina L. Gregory,^a Gregory S. Sulley,^a Leticia Peña Carrodeguas,^a Thomas T. D. Chen,^a Alba Santmarti,^b Nicholas J. Terrill,^c Koon-Yang Lee^b and Charlotte K. Williams^{*a}

^a Chemistry Research Lab, University of Oxford, Mansfield Road, Oxford, UK, OX1 3TA

^b Department of Engineering, Imperial College London, South Kensington, London, UK, SW7 2AZ

^c Diamond Light Source, Harwell Science and Innovation Campus, Didcot, Harwell, UK, OX11 0DE

Table of Contents

1. Additional Experimental details	2
2. Instrumentation	2
3. Catalyst Structure and Synthesis	3
4. Ring-Opening Copolymerization (ROCOP) Steps	4
5. NMR Characterization	5
6. Size-Exclusion Chromatography (SEC)	6
7. DOSY NMR Spectra	11
8. End-group Analysis by ³¹P{¹H} NMR Spectroscopy	12
9. Polymer Purification	13
10. Additional Polymerization Data	14
11. Glass Transition Temperature Data	16
11.1. Differential Scanning Calorimetry (DSC)	17
11.2. Dynamic Mechanical Thermal Analysis (DMTA)	18
12. Mechanical Properties	23
12.1. Uniaxial Extension Tensile Testing	23
12.2. Cyclic Tensile Testing	28
13. Order-to-Disorder Transition	32
14. Thermal Gravimetric Analysis (TGA)	34
15. Small Angle X-ray Scattering (SAXS)	37
16. Degradation Studies	40
17. Comparison to Literature TPEs.	45
18. References	45

1. Additional Experimental details

Phosphorus end group tests: Following a literature procedure,^[1] to polymer (40 mg) dissolved in CDCl₃ (0.4 mL) was added 40 μL of solution containing Cr(acac)₃ (5.5 mg) and internal standard, bisphenol A (400 mg) in pyridine (10 mL) followed by 40 μL of 2-chloro-4,4,5,5-tetramethyl dioxaphospholane.

Degradation experiments: Following the literature,^[2] TBPE-5 (200 mg) was dissolved in toluene (10 mL) before adding *p*-TSA.H₂O (10 mg, 0.05 mmol) and heating with stirring (500 rpm) to 60 °C in a Teflon capped vial. Progress was monitored by NMR and SEC analysis of aliquots taken at various time points. For degradation in distilled H₂O, dumbbell specimens of known mass were placed in water with *p*-TSA.H₂O. At set time points, a specimen was removed, dried under vacuum to constant mass and subject to tensile testing and SEC analysis. For enzymatic hydrolysis investigations at 37 °C, dumbbell specimens were suspended in phosphate buffer solution (pH 7.4) before adding Novozym[®] 51032 (4 wt%) and sodium azide (0.04 wt%) to prevent microbial growth.

2. Instrumentation

NMR: ¹H, ³¹P {¹H} and ¹³C{¹H} NMR were recorded on a Bruker Avance III HD 400 MHz spectrometer. DOSY spectra were recorded on Bruker Avance III HD 500 MHz spectrometer.

Size Exclusion Chromatography (SEC): Polymer (2-10 mg) dissolved in HPLC grade THF (1 mL) were syringe filtered through 2 μm filters before injection into Shimadzu LC-20AD SEC instrument with two PSS SDV 5 μm linear M columns heated to 30 °C. HPLC grade THF was used as the eluent at a flow rate 1.0 mL min⁻¹. RI and UV detectors were calibrated using a series of narrow molecular weight polystyrene standards. Shimadzu SEC post run program was used to analyse the data.

Differential Scanning Calorimetry (DSC): Recorded for precipitated polymer samples on a Mettler Toledo DSC3 Star calorimeter under a N₂ flow (80 mL min⁻¹). Samples were heated to 200 °C and held for 5 minutes, to remove thermal history, before heating and cooling from -80 to 200 °C at a rate of 10 °C min⁻¹. Glass transition temperatures (*T_g*) were determined from the midpoint of the transition in the second heating curve.

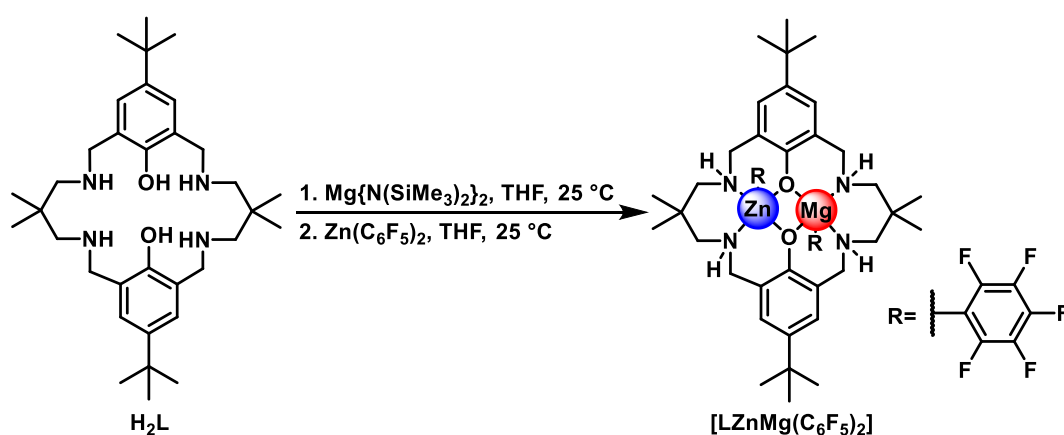
Tensile Testing: Dumbbell specimens were cut according to ISO 527-2, specimen type 5B with Zwick ZCP020 cutting press (length= 35 mm, gauge length = 10 mm, width = 2 mm). Monotonic uniaxial extension experiments were carried out on a Shimadzu EZ-LZ Universal testing instrument at an extension rate of 10 mm min⁻¹. An external camera was used to calculate the Young's Modulus, *E* within the 0.025-0.25% strain region. 10 Specimens were tested for each material. Cyclic tensile tests were conducted to 200% or 1000% strain at a rate of 10 mm min⁻¹. 10 Cycles were measured for each specimen, 3 specimens for each sample.

Dynamic Mechanical Thermal Analysis (DMTA): Recorded on TA instruments RSA-G2 Solids Analyser. Samples were heated with 1 Hz frequency between -60 and 220 °C at a rate of 5 °C min⁻¹.

Thermal Gravimetric Analysis (TGA): Measured on Mettler-Toledo Ltd TGA/DSC 1 system. Powder polymer samples were heated from 30 to 500 °C at a rate of 5 °C min⁻¹, under N₂ flow (100 mL min⁻¹).

Small-angle X-ray Scattering (SAXS): Performed at beamLine station I-22, located at Diamond Light Source, Harwell, United Kingdom. Samples were mounted between two pieces of Kapton[®]. A monochromatic X-ray radiation ($\lambda = 0.1$ nm) and 2D SAXS detector (Pilatus P3-2M, DECTRIS Ltd.) were used for the experiments. 2D scattering patterns were reduced to 1D using Dawn software developed at the Diamond Light Source.^[3] All samples were annealed at 200 °C (above their upper T_g) for 20 mins before being cooled and submitted for SAXS measurements.

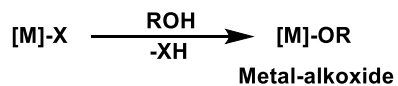
3. Catalyst Structure and Synthesis



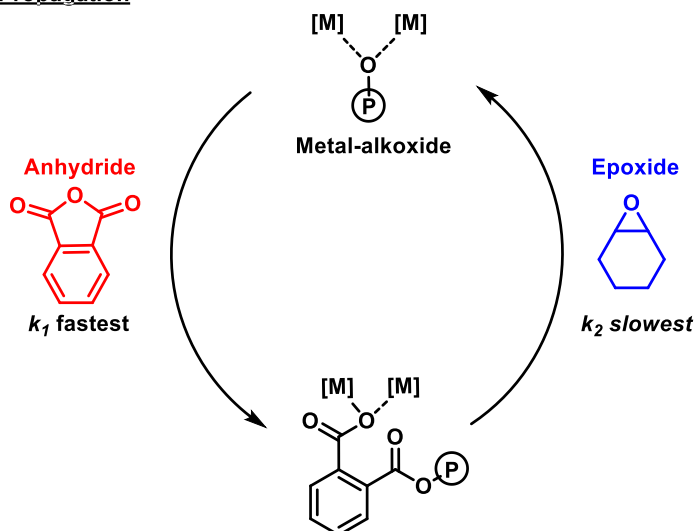
The catalyst was synthesised according to the published procedure.^[4] In a N₂ filled glovebox, $Mg\{N(SiMe_3)_2\}_2$ (0.31 g, 0.90 mmol, 1 equiv.) was added to a solution of H_2L (0.5 g, 0.90 mmol, 1 equiv.) in anhydrous THF (10 mL). The reaction was then left to stir for 1 h before a solution of $Zn(C_6F_5)_2$ (0.36 g, 0.90 mmol, 1 equiv.) in THF (5 mL) was added. The solution was left to stir for 24 h. The precipitated catalyst was then isolated, washed with cold THF (5 mL) and pentane (2 × 5 mL) before being dried to yield a pale orange powder (0.62 g, 70%).

4. Ring-Opening Copolymerization (ROCOP) Steps

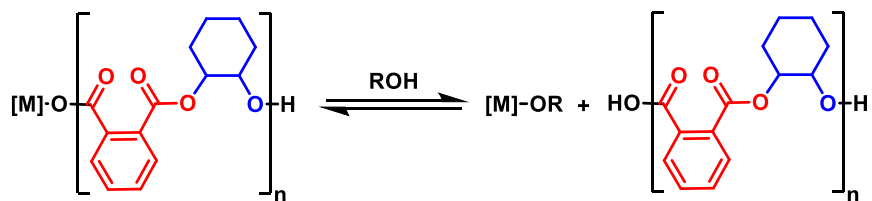
Initiation



Propagation



Chain Transfer Equilibra



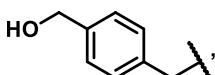
Where X = $-\text{C}_6\text{F}_5$, R = , (P) = propagating chain

Fig. S1 Ring-opening copolymerization (ROCOP) steps.

5. NMR Characterization

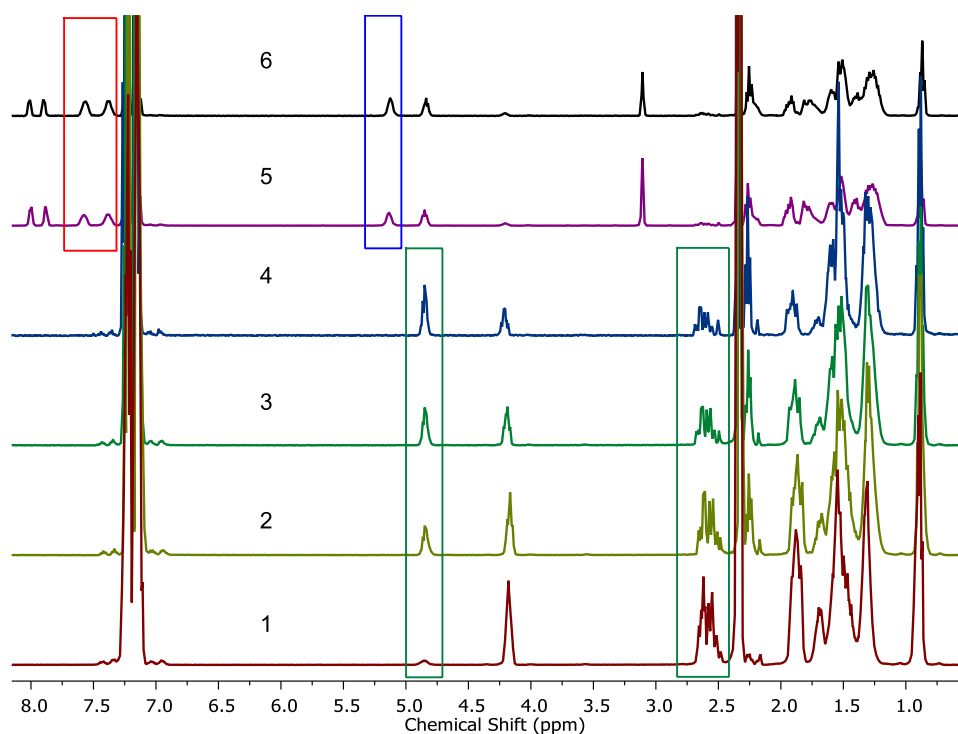


Fig. S2 Stacked ¹H NMR spectra (CDCl₃, 400 MHz) of selected aliquots taken during polymerisation of DL (1-4, green boxes highlight evolution of key PDL environments) and aliquots taken after the addition of PA and CHO mixture (5-6, blue and red boxes highlight CHO and PA environments in polyester (PE) used for conversion determination).

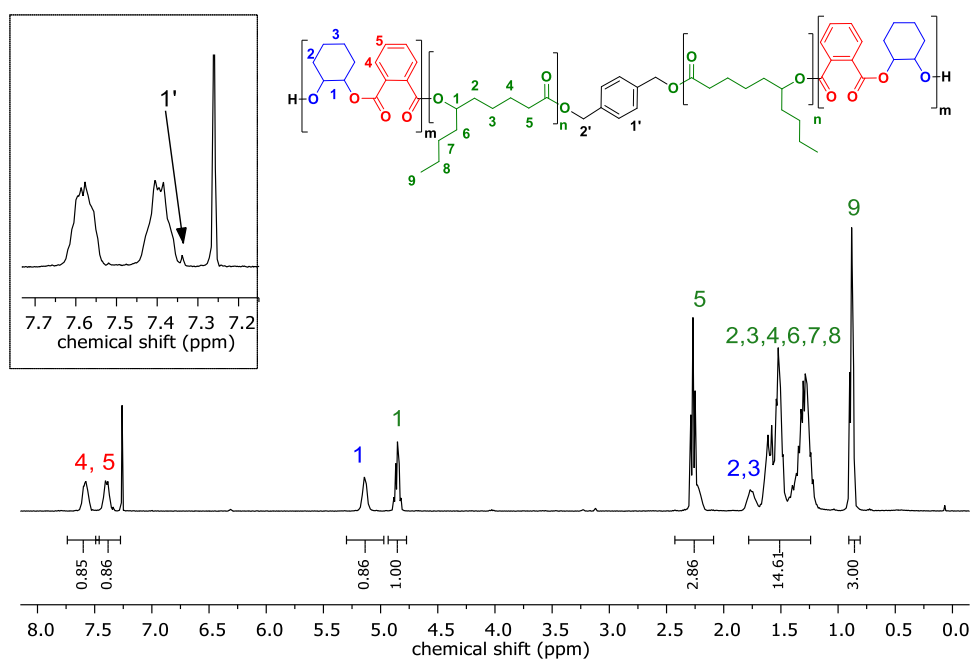


Fig. S3 ¹H NMR spectrum (CDCl₃, 400 MHz) of purified polymer TBPE-3.

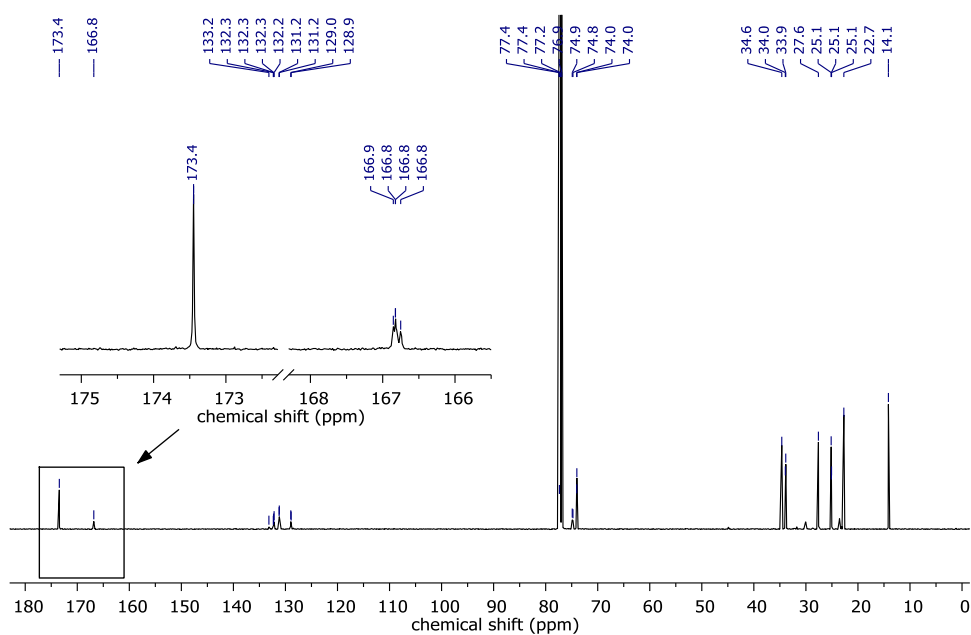


Fig. S4 $^{13}\text{C}\{^1\text{H}\}$ NMR spectrum (CDCl_3) of TBPE-3; inset: carbonyl region showing C=O for PDL at 173.4 ppm and PE (166.8-166.9 ppm) and no evidence of transesterification.

6. Size-Exclusion Chromatography (SEC)

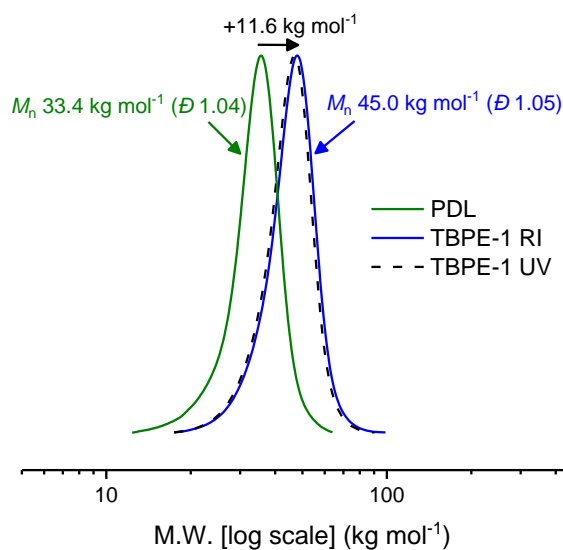


Fig. S5 SEC traces for TBPE-1 (THF eluent, vs. PS standards) showing aliquot taken of reaction mixture before addition of PA/CHO (PDL, green) and of purified triblock copolymer (blue) with RI and UV detectors.

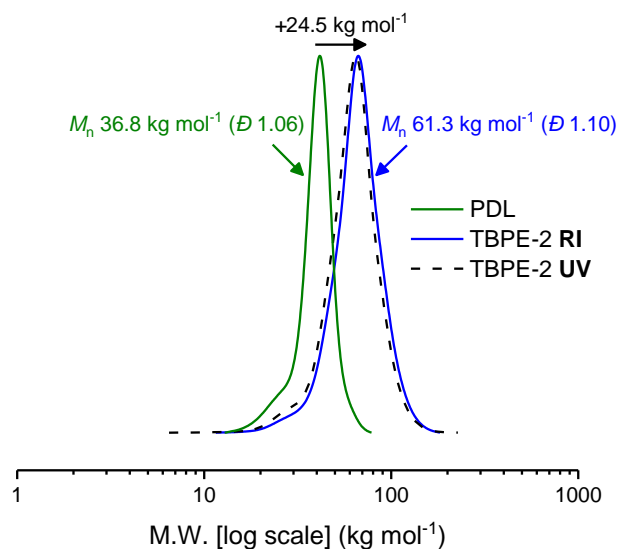


Fig. S6 SEC traces for TBPE-2 (THF eluent, vs. PS standards) showing aliquot taken of reaction mixture before addition of PA/CHO (PDL, green) and of purified triblock copolymer (blue) with RI and UV detectors.

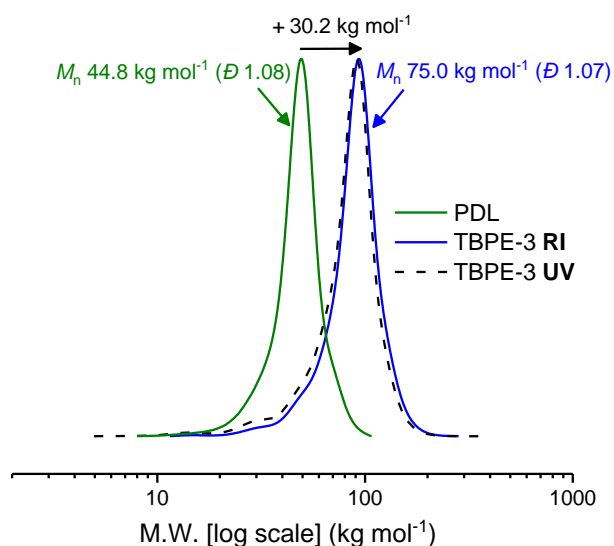


Fig. S7 SEC traces for TBPE-3 (THF eluent, vs PS standards) showing aliquot taken of reaction mixture before addition of PA/CHO (PDL, green) and of purified triblock copolymer (blue) with RI and UV detectors.

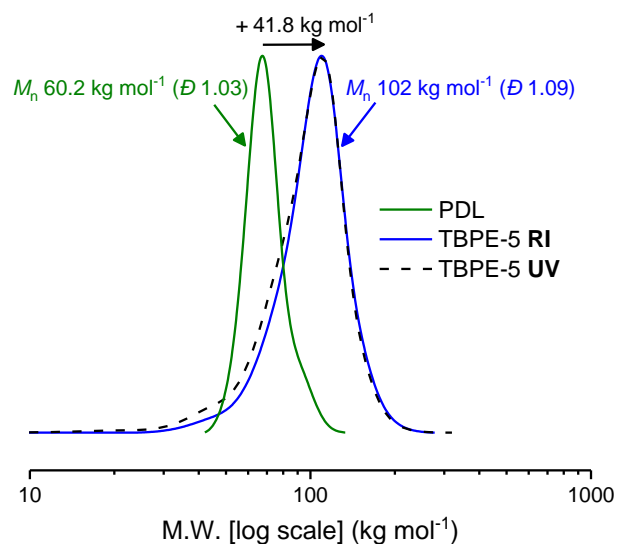


Fig. S8 SEC traces for TBPE-5 (THF eluent, vs. PS standards) showing aliquot taken of reaction mixture before addition of PA/CHO (PDL, green) and of purified triblock copolymer (blue) with RI and UV detectors.

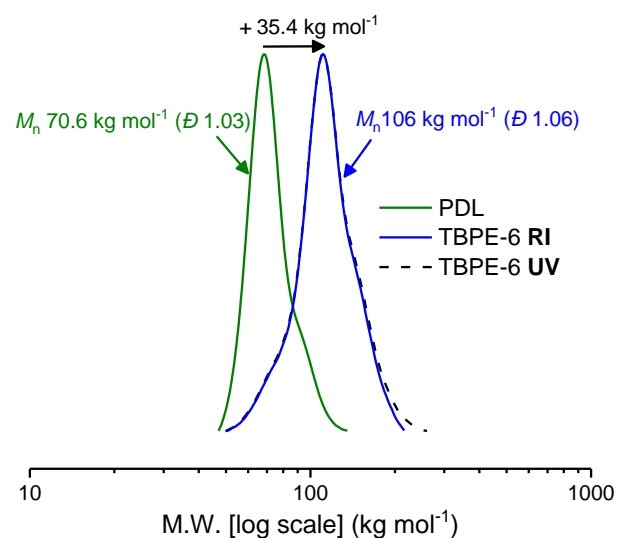


Fig. S9. SEC traces for TBPE-6 (THF eluent, vs. PS standards) showing aliquot taken of reaction mixture before addition of PA/CHO (PDL, green) and of purified triblock copolymer (blue) with RI and UV detectors.

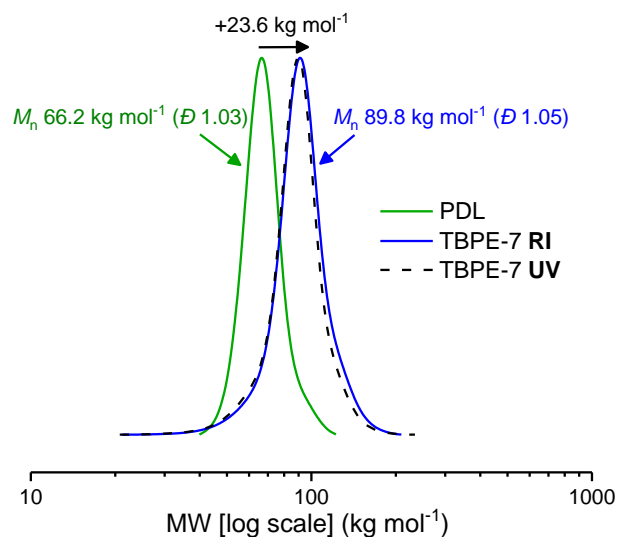


Fig. S10 SEC traces for TBPE-7 (THF eluent, vs PS standards) showing aliquot taken of reaction mixture before addition of PA/CHO (PDL, green) and of purified triblock copolymer (blue) with RI and UV detectors.

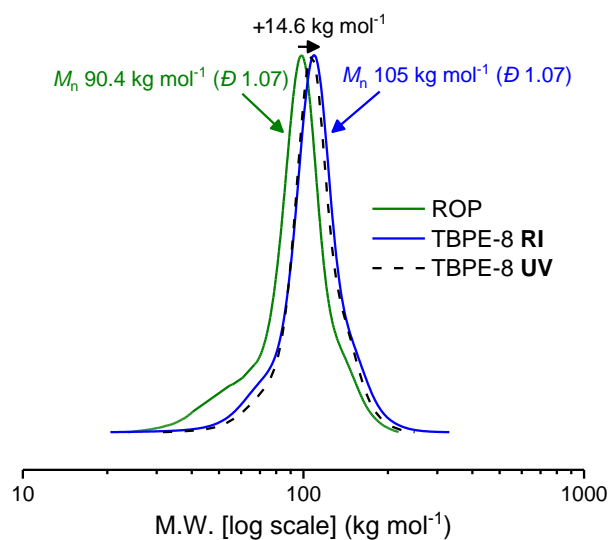


Fig. S11 SEC traces for TBPE-8 (THF eluent, vs PS standards) showing aliquot taken of reaction mixture before addition of PA/CHO (PDL, green) and of purified triblock copolymer (blue) with RI and UV detectors.

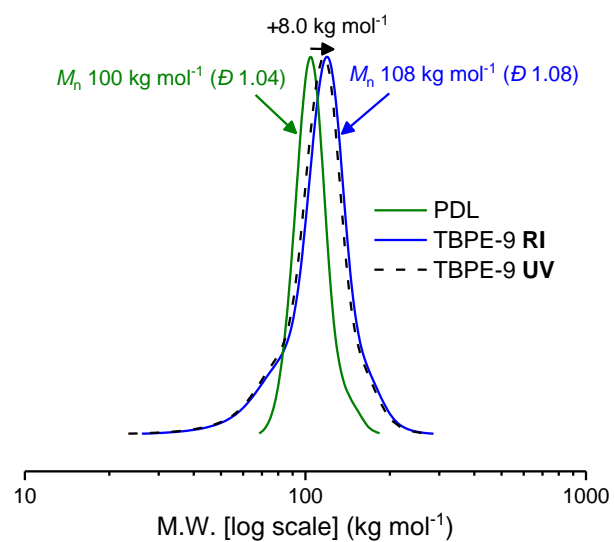


Fig. S12 SEC traces for TBPE-9 (THF eluent, vs PS standards) showing aliquot taken of reaction mixture before addition of PA/CHO (PDL, green) and of purified triblock copolymer (blue) with RI and UV detectors.

7. DOSY NMR Spectra

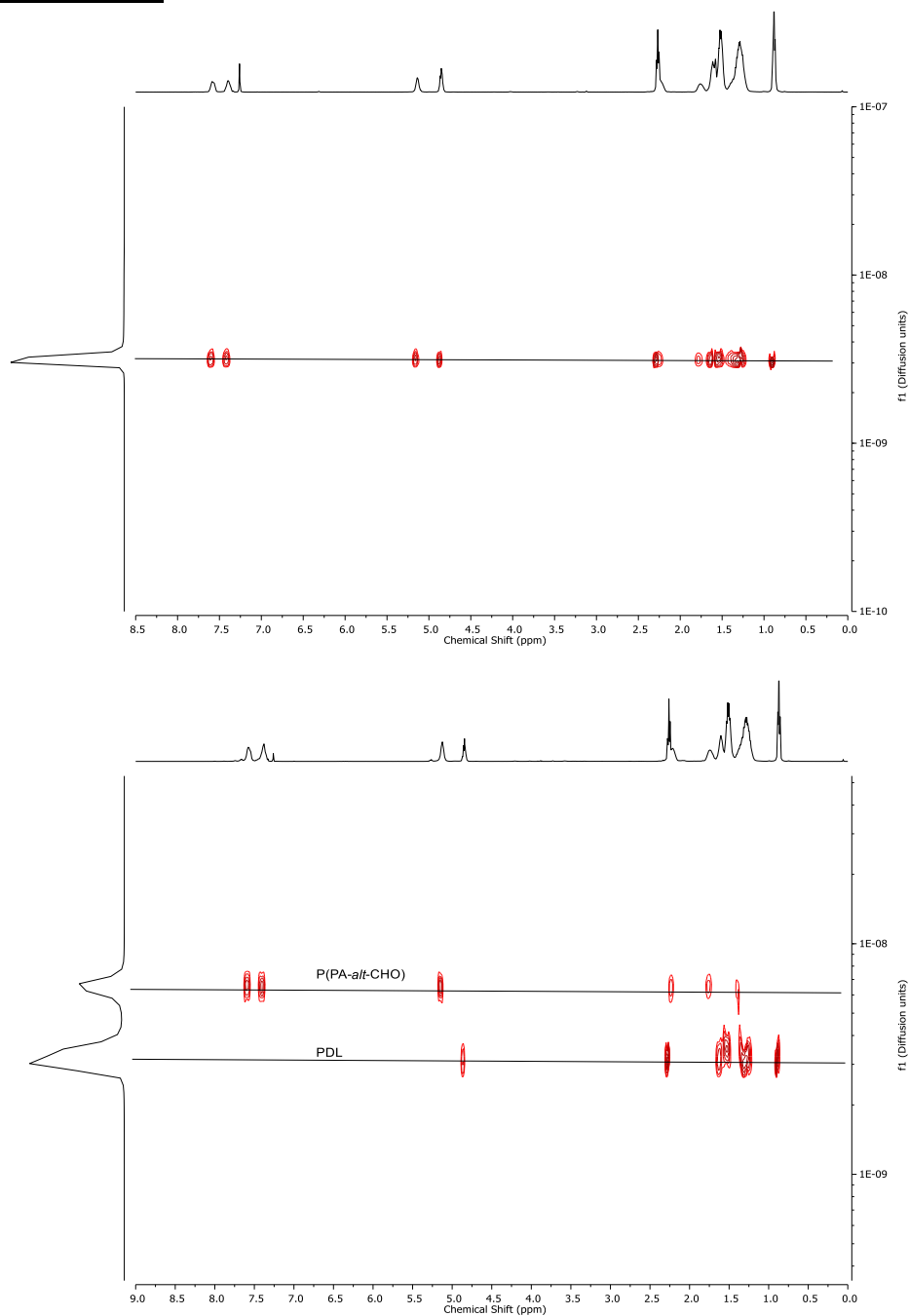


Fig. S13 DOSY NMR spectra (CDCl_3): **Top**; TBPE-3 (M_n 75 kg mol $^{-1}$, D 1.07, $f_{\text{hard}}=0.41$) showing single diffusion coefficient consistent with triblock copolymer formation (*cf.* homopolymer blend). **Bottom**: 50:50 wt% blend of PDL and P(PA-*alt*-CHO) showing two diffusion coefficients.

8. End-group Analysis by $^{31}\text{P}\{^1\text{H}\}$ NMR Spectroscopy

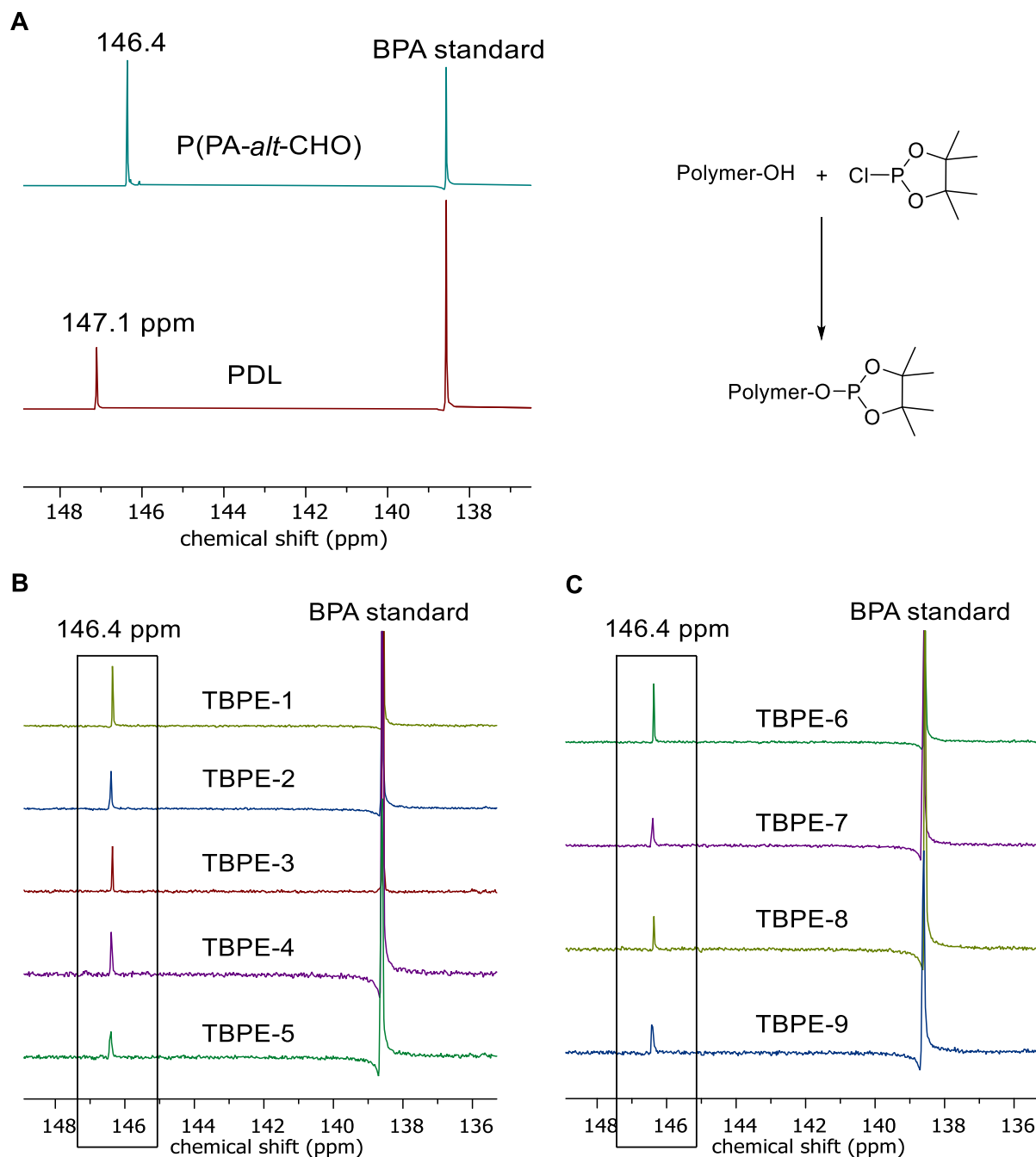


Fig. S14 $^{31}\text{P}\{^1\text{H}\}$ NMR spectra (CDCl_3) after reaction of polymer hydroxyl end groups with 2-chloro-4,4,5,5-tetramethyldioxaphospholane (see experimental details above) showing **A**: PE and PDL polymers for reference, **B**: $f_{\text{hard}} \sim 0.4$ series (TBPE-1 to -5) and **C**: series with $M_n \sim 100 \text{ kg mol}^{-1}$ (TBPE-6 to -9). The peak at 138.6 ppm is used as the internal standard and corresponds to the product of the reaction between the phosphorous reagent and bis-phenol A (BPA).

9. Polymer Purification

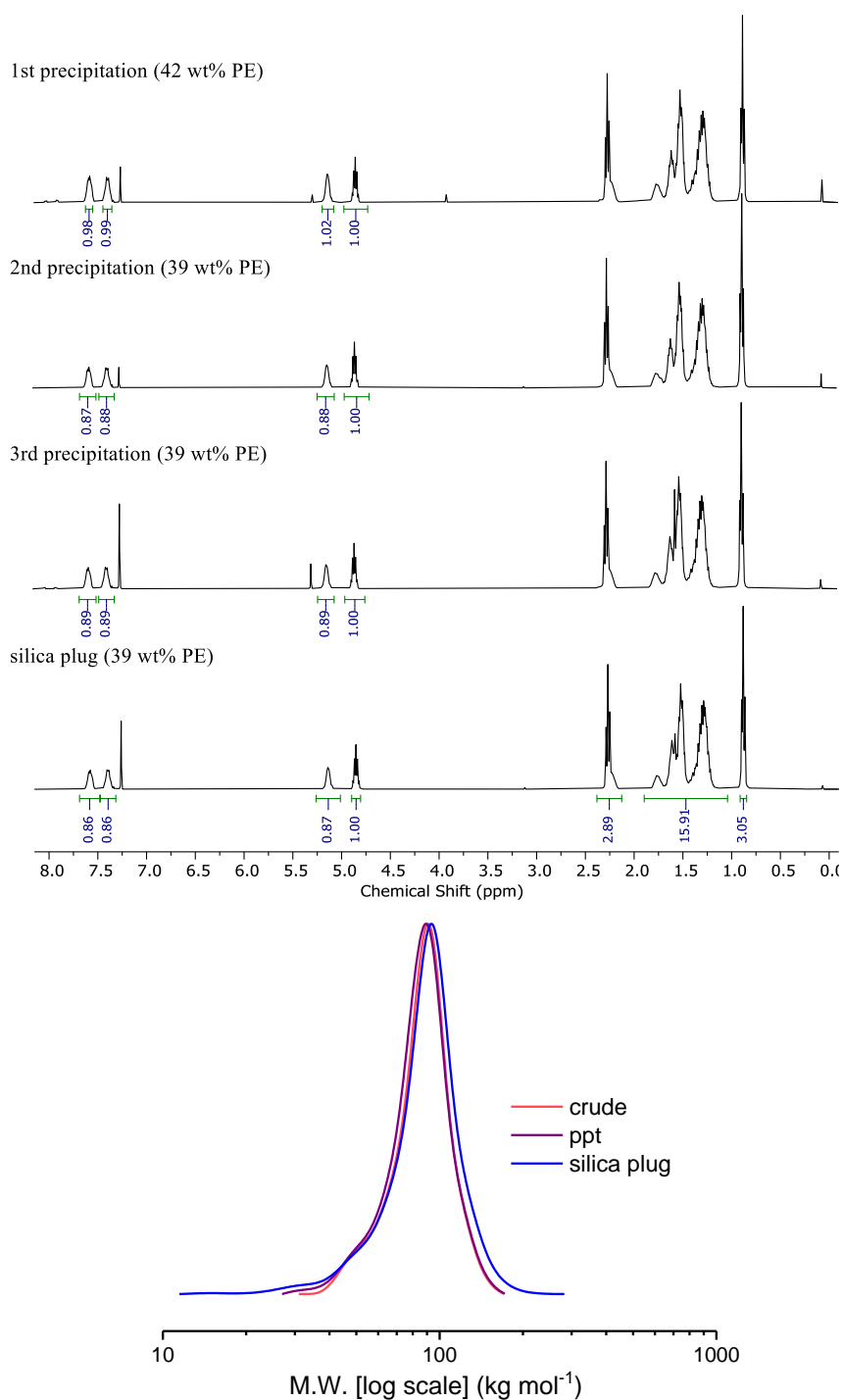


Fig. S15 ¹H NMR spectra and SEC analysis of purified polymer TBPE-3 samples. Purification was by precipitation from MeOH and passing through a silica plug. **Top:** ¹H NMR spectra (CDCl₃) after various purification steps. The wt% PE is determined by relative integration of the PDL methine signal (4.85 ppm, 1H) and CHO in PE (5.14 ppm, 2H). The reduction in wt% from 42 to 39 wt%, after the first precipitation, is attributed to errors within this wt% measurement method (typically NMR error range = ±5%). **Bottom:** TBPE-3 SEC traces (THF eluent, RI detector) of the crude reaction mixture, TBPE-3 after precipitation from methanol and the TBPE-3 film formed following purification by passing through a silica plug.

10. Additional Polymerization Data

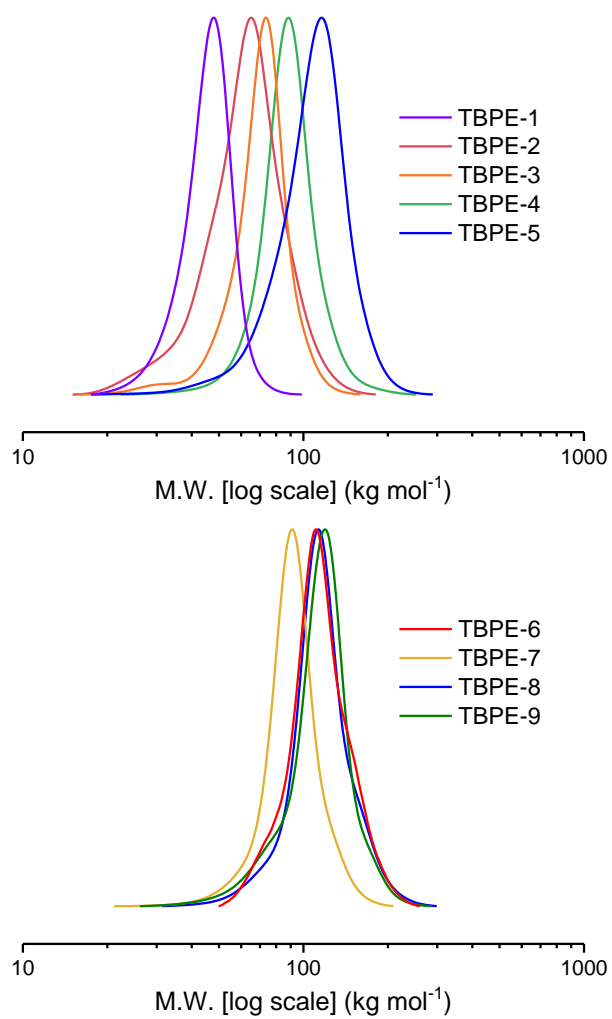


Fig. S16 Stacked SEC traces of polymer films, $f_{\text{hard}} \sim 0.4$ series (top) and $M_n \sim 100 \text{ kg mol}^{-1}$ (bottom).

Table S1. Polymerisation Data for TBPEs.^a

Sample	PDL				PE- <i>b</i> -PDL- <i>b</i> -PE				
	Conv. (%) ^b	[M] ₀ / [I] ₀	M _{n, calc} (kg mol ⁻¹) ^c	M _{n, SEC} (kg mol ⁻¹) [Đ] ^d	Conv. PA (%) ^e	M _{n, calc} (kg mol ⁻¹) ^f	M _{n, NMR} (kg mol ⁻¹) ^g	M _{n, SEC} (kg mol ⁻¹) [Đ] ^h	wt% PE ⁱ
TBPE-1	90	200	32.7	33.4 [1.04]	96	53.4	43.7	45.0 [1.05]	38
TBPE-2	98	200	33.4	36.8 [1.06]	98	54.8	59.2	61.3 [1.10]	42
TBPE-3	97	250	41.3	44.8 [1.08]	87	78.8	73.5	75.0 [1.07]	39
TBPE-4	99	250	42.1	48.4 [1.08]	99	84.8	80.3	85.3 [1.06]	42
TBPE-5	92	400	62.7	60.2 [1.03]	85	99.3	95.4	102 [1.09]	38
TBPE-6	99	400	67.4	70.6 [1.03]	87	94.2	95.0	106 [1.06]	27
TBPE-7	95	400	64.7	66.2 [1.03]	89	97.6	88.3	89.8 [1.05]	23
TBPE-8	99	600	97.0	90.4 [1.07]	99	100.7	113.5	105 [1.07]	18
TBPE-9	99	600	97.0	100.0 [1.04]	99	100.7	102.0	108 [1.08]	11

^a Reaction conditions: 80 °C, [DL]₀ = 1.7 M in toluene; ^b Determined from the relative integrals in ¹H NMR spectra of methane resonances at 4.31 and 4.85 ppm for DL and PDL, respectively; ^c Based on initial [S]₀/[BDM]₀ ratio and % conv. DL; ^d Estimated by SEC (THF eluent, RI detector vs. PS standards) of aliquot taken prior to addition of PA/CHO; ^e Conversion PA to PE determined from the relative integrals of resonances for PA (8.15 ppm) compared to PE (7.71 ppm) from the ¹H NMR spectrum, no ether linkages; ^f Based on initial [PA+CHO]₀/[BDM]₀ ratio and % conv. PA; ^g Estimated from the relative integrals of PE (7.51 ppm) and PDL (4.79 ppm) resonances in the ¹H NMR spectra of the purified polymer films; ^h Estimated by SEC of purified polymer films (RI and UV detector, THF eluent vs PS standards. ⁱ Determined from the relative integrals of PE (7.51 ppm) and PDL (4.79 ppm) resonances in the ¹H NMR spectra of purified polymer films and using molar masses of PDL and PE repeat units of 170.3 and 246.3 g mol⁻¹, respectively.

**Fig. S17** Transparent colourless films of TBPEs.

Calculation of the volume fraction of the hard (PE) domain (f_{hard}):

$$f_{hard} = \frac{\rho_{hard}}{\rho_{PDL} \left(\frac{1}{\omega_{hard}} - 1 \right) + \rho_{hard}} \quad (1)$$

Where ω_{hard} is the wt% of hard block determined from the integrals in the 1H NMR spectrum (see Table S1) and ρ_{PDL} , ρ_{PE} are the densities of PDL and PE at room temperature, respectively.

Degree of polymerisation relative to a standard reference volume (N):

$$N_{PDL} = \frac{M_{PDL}}{\rho_{PDL}(T)N_A v_{ref}}; N_{total} = N_{PDL} + N_{hard} \quad (2)$$

Where N_{PDL} , N_{hard} and N_{total} are the degrees of polymerisation relative to a standard reference volume ($v_{ref}=118 \text{ \AA}$) for PDL, the PE hard domain and overall, respectively. N_A is Avogadro's number.

11. Glass Transition Temperature Data

Table S2. Summary of TBPE thermal properties measured by DSC and DMTA.

Sample	DP PE-PDL- PE ^a	DSC ^b				DMTA ^e			OTW ^f
		$T_{g,PDL}$ (°C)	$T_{g,PDL}^{calc}$ (°C) ^c	$T_{g,PE}$ (°C)	$T_{g,PE}^{calc}$ (°C) ^d	$T_{g, PDL}$ (°C)	$T_{g, PE}$ (°C)	T_{ODT} (°C)	
PE	41	-		130		-	-	n.a.	
PE	20	-		122		-	-	n.a.	
PDL	352	-51		-		-	-	n.a.	
TBPE-1	35-164-35	-49	-52	105	111	nd	124	158	173
TBPE-2	52-209-52	-50	-51	122	123	nd	142	175	192
TBPE-3	59-269-59	-50	-51	123	126	nd	143	183	193
TBPE-4	73-292-73	-50	-51	126	130	nd	145	187	195
TBPE-5	79-371-79	-51	-51	138	131	nd	155	193	206
TBPE-6	58-455-58	-51	-51	nd	125	-42	146	n.o.	188
TBPE-7	42-406-42	-51	-51	nd	117	-41	136	n.o.	177
TBPE-8	38-506-38	-51	-51	nd	114	-44	132	n.o.	176
TBPE-9	24-565-24	-51	-51	nd	95	-44	123	n.o.	167

^a Degree of polymerization (DP) determined from overall M_n estimated by SEC and wt% hard domain from 1H NMR spectra integrals as described in Table 1 and S1; ^b T_g values estimated by DSC, heating rate $10 \text{ }^\circ\text{C min}^{-1}$, second heating curve; ^c Determined using the Flory-Fox equation: $T_g = T_g^\infty - \frac{K}{M_n}$, using parameters reported by Hillmyer and coworkers ($K = 3400 \pm 2200$, $T_g^\infty = 51.4 \pm 0.3^\circ\text{C}$).^[6] ^d Flory-Fox parameters ($T_g^\infty = 147 \pm 10 \text{ }^\circ\text{C}$ and $K = 305 \pm 74 \text{ kg mol}^{-1}$) estimated based on T_g values measured in this work and those reported for the M_n range 4.0 to 34.6 kg mol^{-1} (a total of 20 data points) with $T_g \sim 57$ to $146 \text{ }^\circ\text{C}$.^[7] All data was recorded at $10 \text{ }^\circ\text{C min}^{-1}$ from the second cycle, samples show $< 1 \%$ ether linkages. NB. It remains a challenge within the field to achieve high M_n PE limiting the accuracy of these parameters. ^e Measured from the peak in $\tan(\delta)$, 1 Hz frequency, $5 \text{ }^\circ\text{C min}^{-1}$ heating rate, 0.1 N pre-load, 0.1 % stain for entries TBPE-1 to 5, 1% strain for TBPE-6 to-9. The glass transition temperatures determined by DSC are systematically about $20 \text{ }^\circ\text{C}$ lower for PE compared to those measured by DMTA. This is a well reported observation and attributed to different heating rates, frequency and means of measuring the T_g value from the data (i.e midpoint of glass transition from DSC and peak in $\tan(\delta)$ by DMTA).^[8] n.d.=not determined, n.o.=not observed, n.a.= not applicable. ^f Theoretical operating temperature window (OTW) based on upper and lower glass transition temperatures determined by DSC for TBPE-1 to -5 and DMTA for -6 to -9.

11.1. Differential Scanning Calorimetry (DSC)

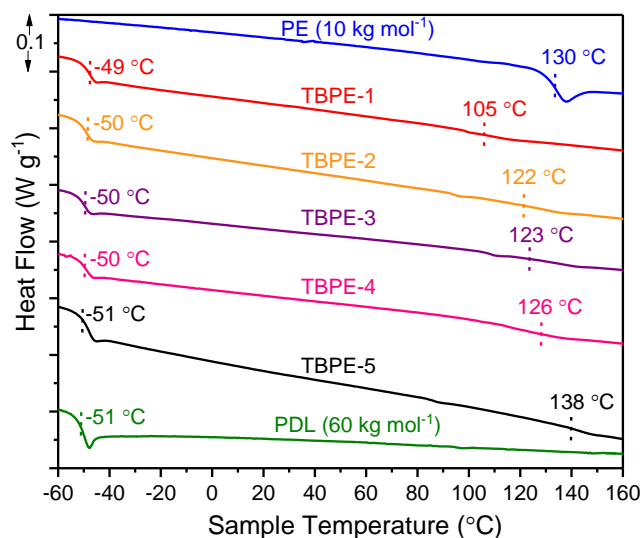


Fig. S18 DSC traces (second heating curve) of purified TBPE-1 to -5 and pure PDL and PE heated at a rate of 10 °C min^{-1} from -80 to 200 °C .

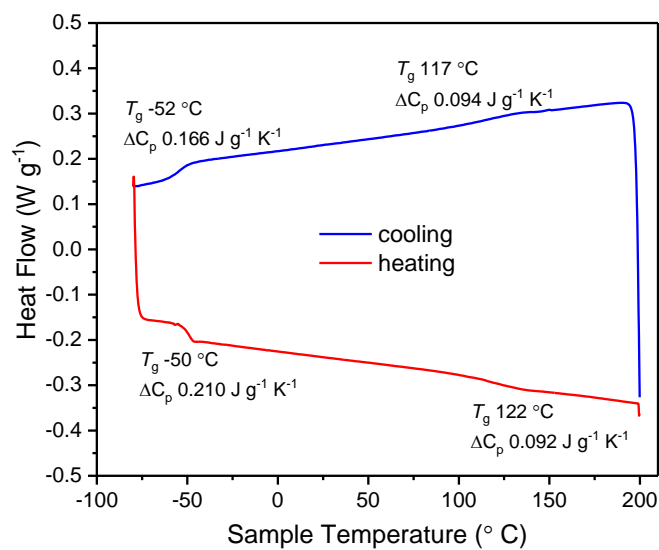


Fig. S19 DSC second heating and cooling for TBPE-2. Heating rate, 10 °C min^{-1} , -80 to 200 °C , N_2 flow.

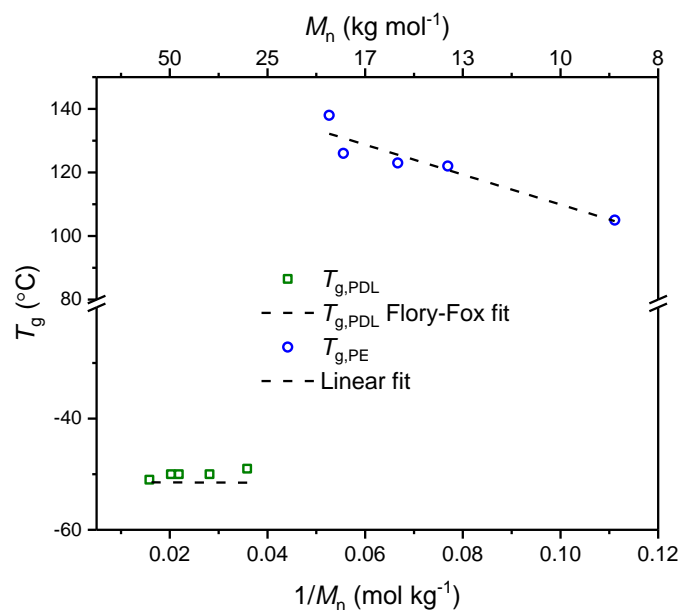


Fig. S20 Dependence of glass transition temperature (T_g) on molar mass for PDL (\square) and PE (\circ) domains for TBPE-1 to -5. Temperatures were measured by DSC (at a heating rate of $10\text{ }^\circ\text{C min}^{-1}$) from the midpoint of the glass transition in the second heating curve. Dashed line is Flory-Fox fit for PDL homopolymer $T_g = T_g^\infty - \frac{K}{M_n}$ where $T_g^\infty = 51.4 \pm 0.3\text{ }^\circ\text{C}$ and $K = 3400 \pm 2200\text{ kg mol}^{-1}$.^[6]

11.2. Dynamic Mechanical Thermal Analysis (DMTA)

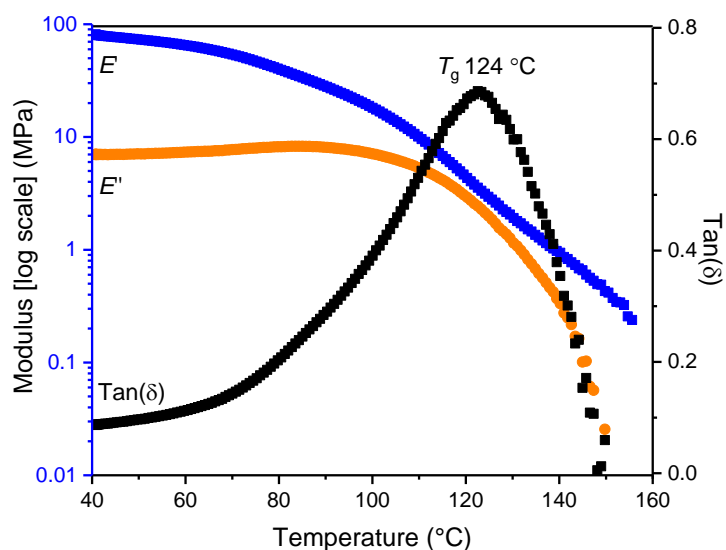


Fig. S21 DMTA of TBPE-1 (1 Hz frequency, heating rate $5\text{ }^\circ\text{C min}^{-1}$, 1% amplitude strain, 0.1 N pre-load).

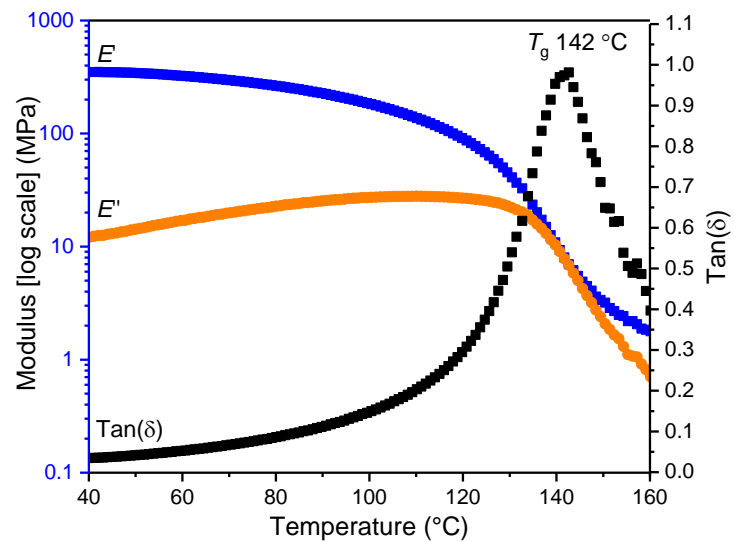


Fig. S22 DMTA of TBPE-2 (1 Hz frequency, heating rate 5 °C min⁻¹, 0.1% amplitude strain, 0.1 N pre-load).

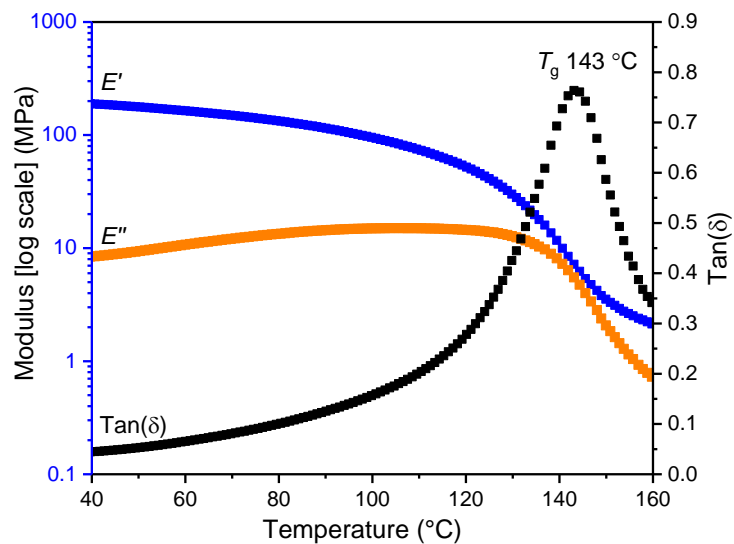


Fig. S23 DMTA of TBPE-3 (1 Hz frequency, heating rate 5 °C min⁻¹, 1% amplitude strain, 0.1 N pre-load).

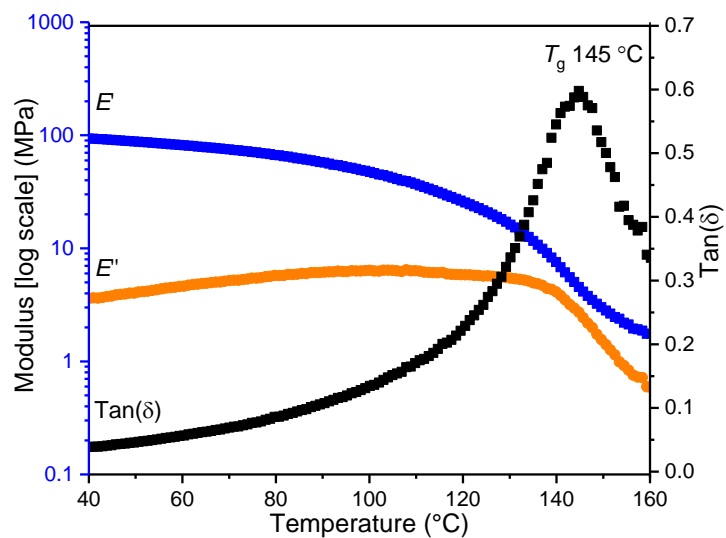


Fig. S24 DMTA of TBPE-4 (1 Hz frequency, heating rate 5 °C min⁻¹, 0.1% amplitude strain, 0.1 N pre-load).

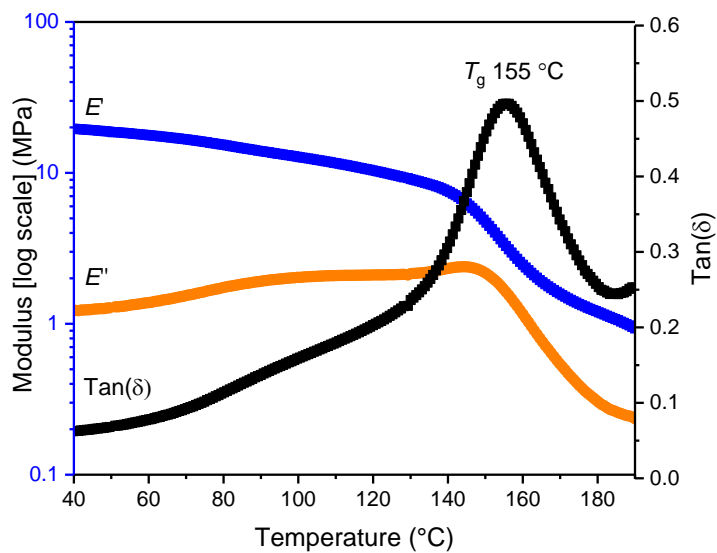


Fig. S25 DMTA of TBPE-5 (1 Hz frequency, heating rate 5 °C min⁻¹, 1% amplitude strain, 0.1 N pre-load).

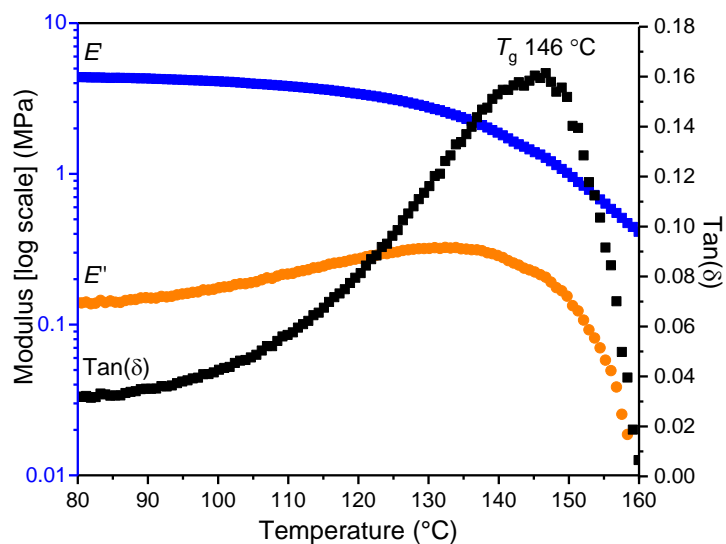


Fig. S26 DMTA of TBPE-6 (1 Hz frequency, heating rate 5 °C min⁻¹, 0.1% amplitude strain, 0.1 N pre-load).

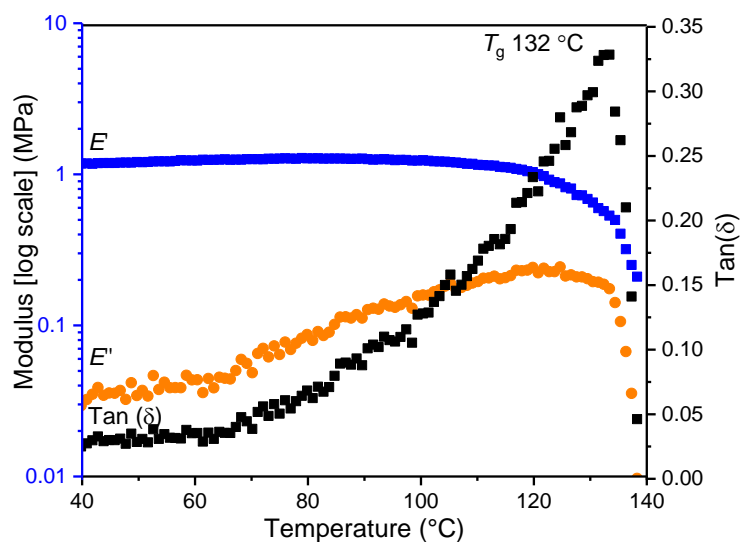


Fig. S27 DMTA of TBPE-8 (1 Hz frequency, heating rate 5 °C min⁻¹, 0.1% amplitude strain, 0.1 N pre-load).

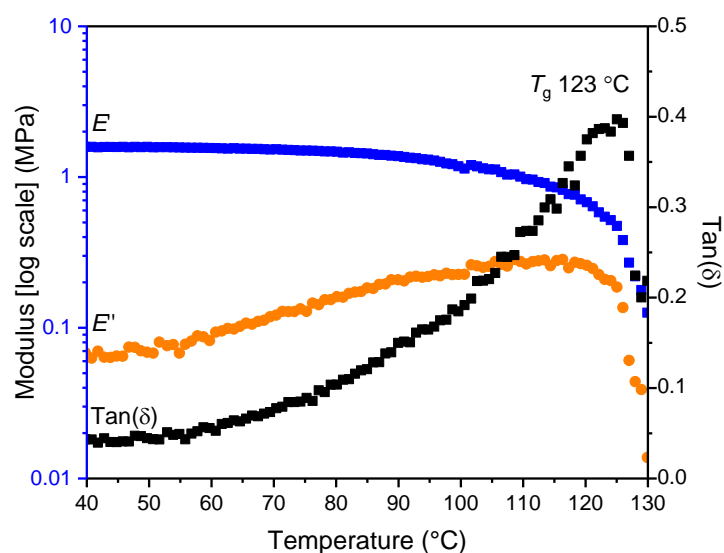


Fig. S28 DMTA of TBPE-9 (1 Hz frequency, heating rate 5 °C min⁻¹, 0.1% amplitude strain, 0.1 N pre-load).

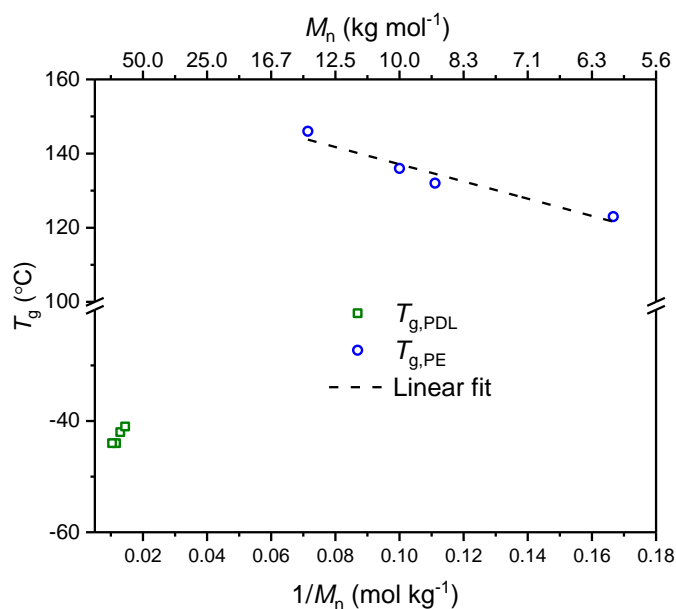


Fig. S29 Dependence of glass transition temperature (T_g) on molar mass of PE (o) and PDL (□) domains for TBPE-6 to -9. T_g values determined by DMTA from peak maxima in $\tan(\delta)$.

Table S3. Calculation of M_e for TPBE-6 to -9 and comparison to literature values.

Triblock Copolymer ^a	G' (MPa) ^b	M_e^{PDL} (kg mol ⁻¹) ^c	M_e^{PDL} (kg mol ⁻¹)	Reference
TBPE-6 (106, 0.29)	2.3	1.1	2.9	This work
TBPE-7 (90, 0.24)	1.1	2.3	5.5	This work
TBPE-8 (105, 0.19)	0.5	5.3	9.0	This work
TBPE-9 (108, 0.12)	0.4	5.7	9.1	This work
PLA-PDL-PLA (136, 0.27)		5.3		[6]
PLA-PDL-PLA (148, 0.21)		6.7		[6]
PLLA-PDL-PLLA (162, 0.063)	0.63		4.6	[9]
PLLA-PDL-PLLA (173, 0.13)	0.97		3.9	[9]

PLLA-PDL-PLLA (191, 0.24)	1.24		4.8	[9]
PLA-PDL-PLA (140, * 0.25)	0.83		7.2	[9]

^a Name of polymer (total M_n by SEC, f_{hard}), ^{*} Theoretical M_n from monomer-to-initiator loading; ^b Shear storage modulus which is related to the storage modulus E' by: $E' = 2G'(1+\nu)$, assuming a Poisson's ratio (ν) of 0.5, typical of elastomers. ^c Molecular weight between entanglements (M_e) Calculated from the following relationship: $M_e^{PDL} = \frac{\rho RT}{G'}$ where ρ is the density of PDL. ^d Calculated using the Guth-Smallwood equation: $M_e^{PDL} = \rho RT / G(1 + 2.5f_{hard} + 14.1f_{hard}^2)$, which assumes spherical hard domains acting as rigid fillers.^[10]

12. Mechanical Properties

12.1. Uniaxial Extension Tensile Testing

Length = 35 mm, gauge length = 10 mm, width = 2 mm.

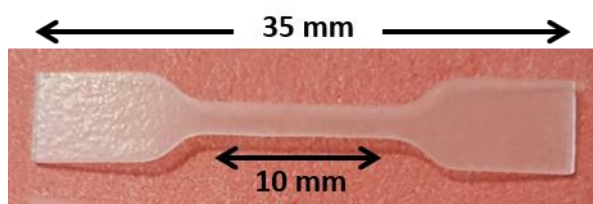


Table S4. Mechanical properties for TBPE-1 to -5 containing ca. 40 wt% PE. Comparison to commercial styrenic block copolymers has been made alongside literature examples with PDL midblock.^a

Sample	σ_y (MPa) ^c	ϵ_y (%) ^c	E_y (MPa) ^d	E' (MPa) ^e	σ_b (MPa) ^f	ϵ_b (%) ^f
TBPE-1	2.7 ± 0.2	4.6 ± 0.8	48 ± 6	54	13.3 ± 4.2	1110 ± 92
TBPE-2	4.5 ± 0.3	4.0 ± 0.7	226 ± 8	283	29.1 ± 4.4	1079 ± 128
TBPE-3	3.1 ± 1.0	3.7 ± 1.2	165 ± 21	194	16.6 ± 0.9	1060 ± 49
TBPE-4	2.9 ± 1.2	8.4 ± 3.3	68 ± 7	96	12.5 ± 1.2	1362 ± 121
TBPE-5	1.6 ± 0.7	12.1 ± 3.8	18 ± 3	20	16.5 ± 1.0	1342 ± 43

^a Unless otherwise noted, mechanical properties were measured by uniaxial tensile testing experiments of solvent cast films at extension rate of 10 mm min⁻¹; reported values are a mean of 10 specimens, error is standard deviation. Stress is measured as $\sigma = F/A_0$ where F = load, A_0 original cross-sectional area of specimen (engineering stress) and strain $\epsilon = \Delta l/l_0$; l_0 original length of specimen (engineering strain). ^b Determined from overall M_n by SEC and wt% PE; ^c Stress and strain at the yield point. ^d Young's Modulus measured as ratio of stress to strain in linearly elastic region following Hooke's Law $\sigma = E\epsilon$; determined by external camera in 0.025-0.25% elongation region; measure of stiffness of material; ^e Storage modulus (E') measured by DMTA for comparison with Young's Modulus (E). E is systematically lower than E' which is attributed to solvent cast vs. thermally pressed samples and error in determining E from stress-strain curve. ^f Maximum stress before break/fracture of material and percent elongation to break (ultimate elongation).

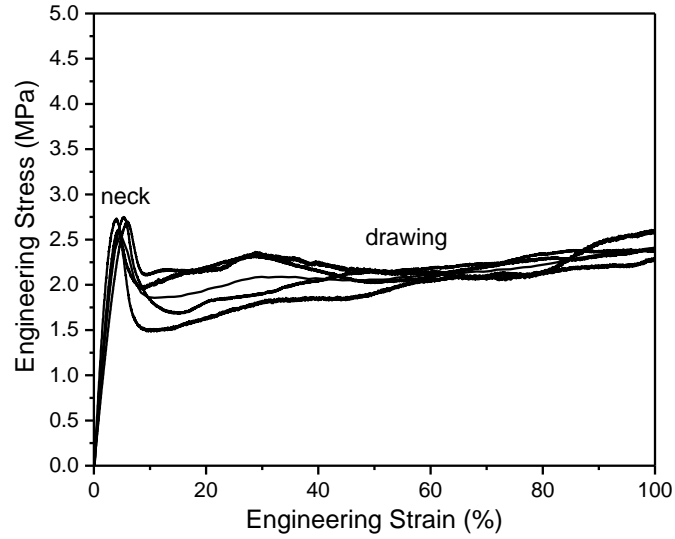


Fig. S30 Stress-Strain curves for TBPE-1 (10 mm min^{-1} extension rate).

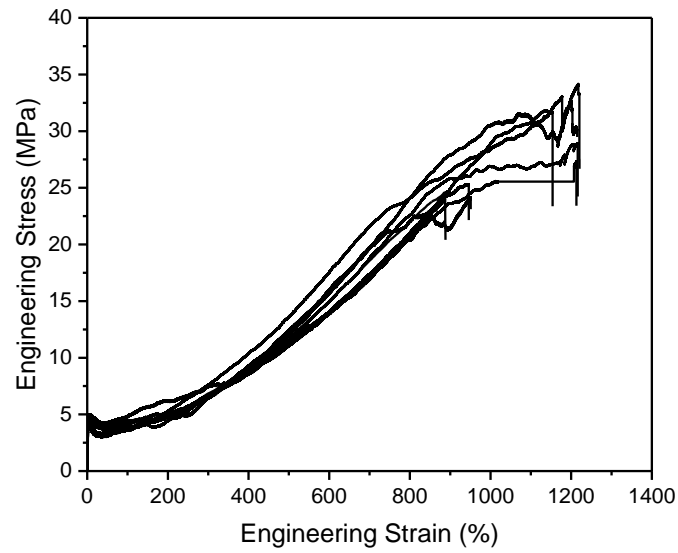


Fig. S31 Stress-Strain curves for TBPE-2 (10 mm min^{-1} extension rate).

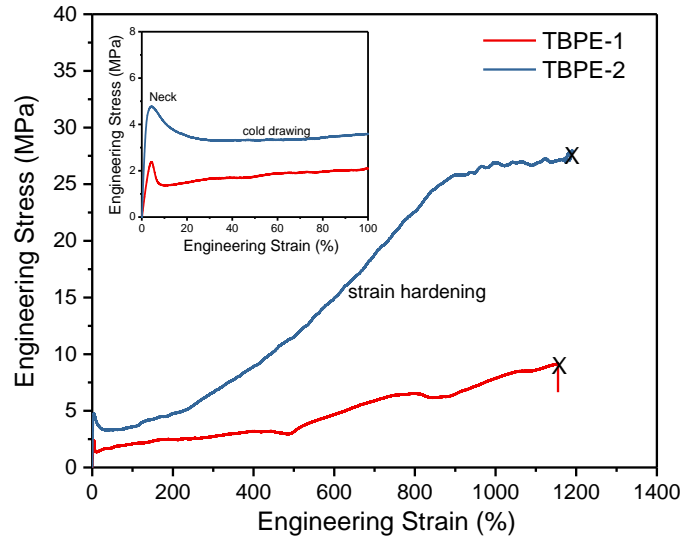


Fig. S32 Representative stress-strain curves for TBPE-1 and TBPE-2 for direct comparison. Inset: 0-100% strain region showing neck and cold drawing.

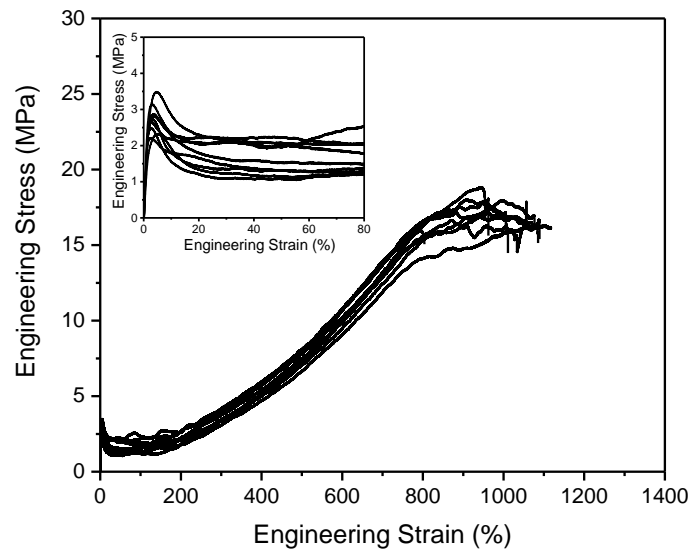


Fig. S33 Stress-Stress curves for TBPE-3 (10 mm min^{-1} extension rate). Inset; 0-80% elongation region showing yield point.

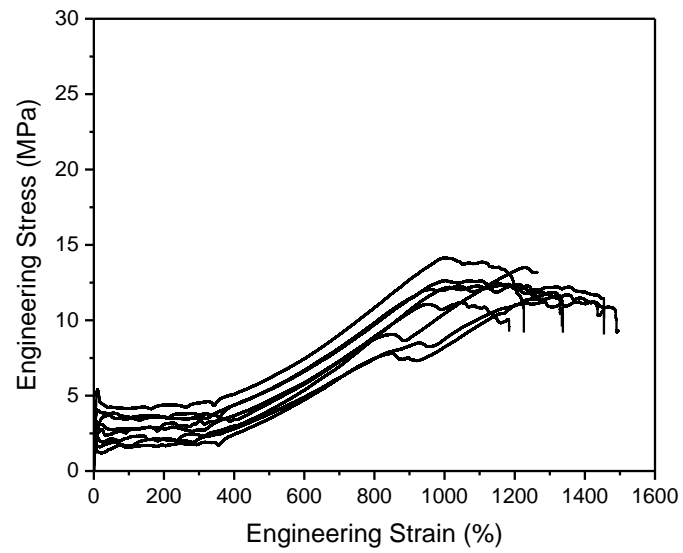


Fig. S34 Stress-Stress curves for TBPE-4 (10 mm min^{-1} extension rate).

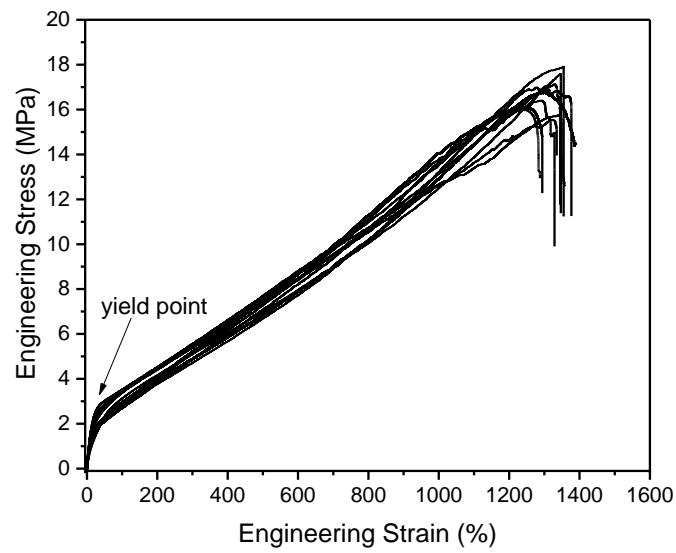


Fig. S35 Stress-Stress curves for TBPE-5 (10 mm min^{-1} extension rate).

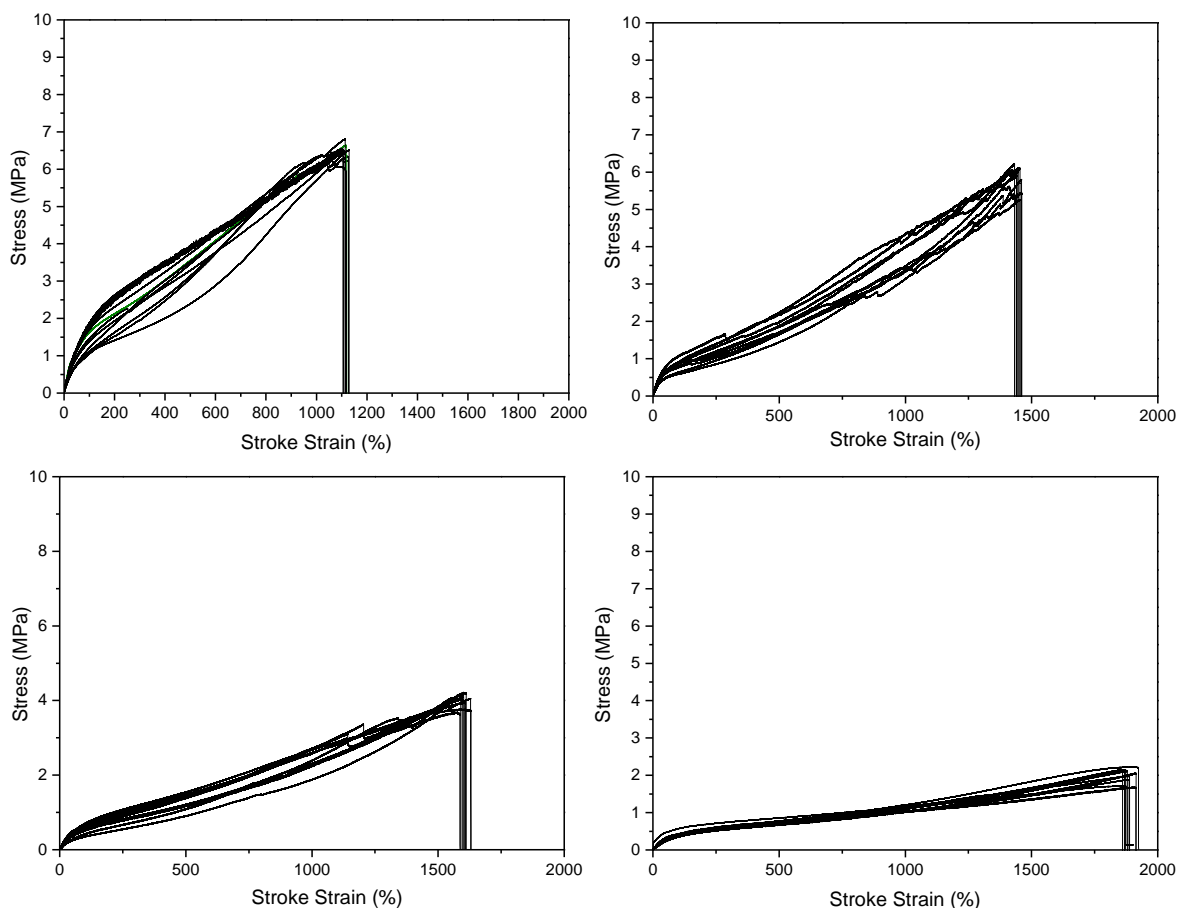


Fig. S36 Stress strain curves TBPEs-6 to -9 (extension rate 10 mm min^{-1}). **Top-left to right:** TBPE-6 and TBPE-7; **Bottom-left to right:** TBPE-8 and TBPE-9.

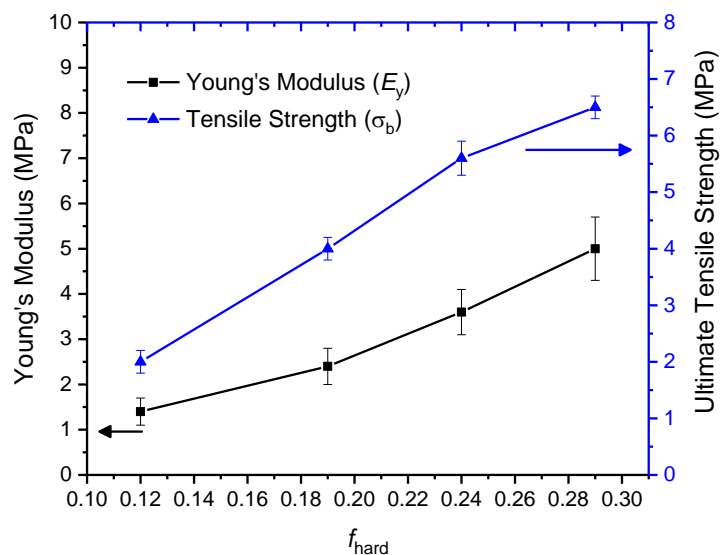


Fig. S37 Young's Modulus and ultimate tensile strength as a function of volume fraction of hard block for TBPE-6 to 9. Error bars represent the standard deviation of measurements carried out on 10 specimens cut from solvent cast films.

12.2. Cyclic Tensile Testing

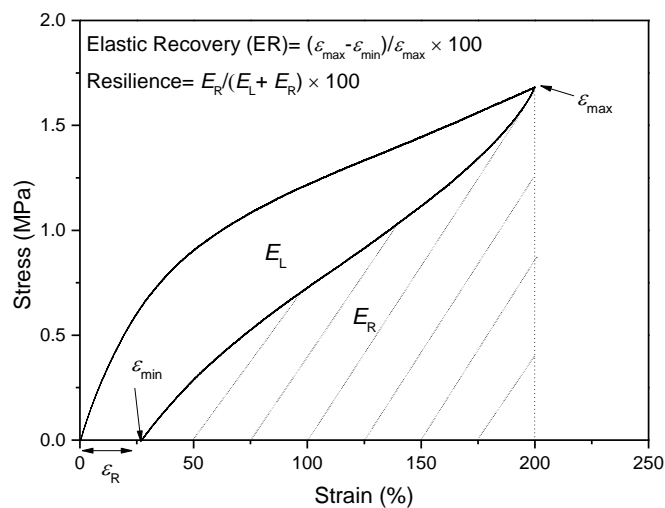


Fig. S38 Schematic of parameters measured during cyclic tensile test. Calculation of elastic recovery and resilience where E_L is energy loss, E_R energy recovery, ϵ_{max} (maximum strain), ϵ_{min} (minimum strain), ϵ_R residual strain. Reproduced from C. Tang and coworkers.^[11]

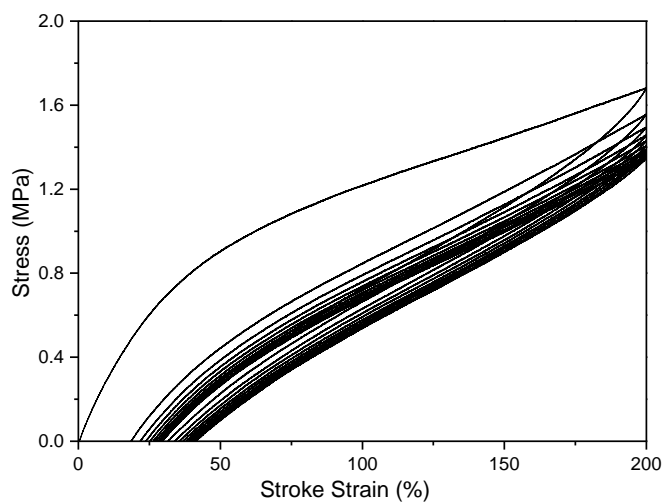


Fig. S39 Stress-Strain curve for a cyclic tensile test of TBPE-6 sample tested for 10 cycles to a maximum strain of 200% strain at a rate of 10 mm min^{-1} .

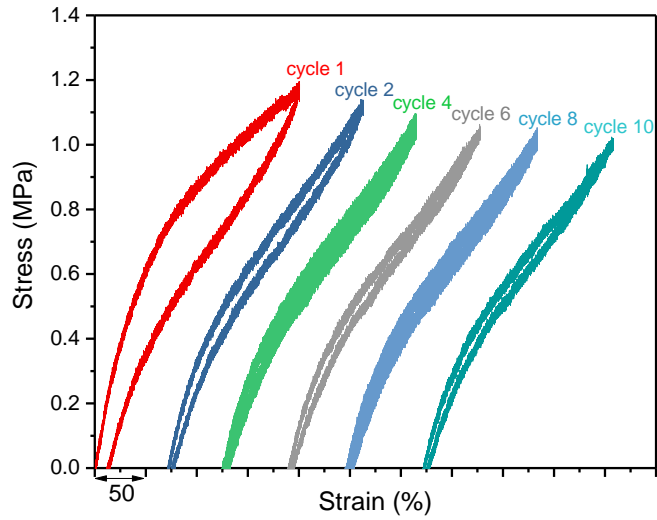


Fig. S40 Cyclic tensile test for TBPE-7 to 200 % strain (10 mm min^{-1}) showing alternate cycles, horizontally shifted for clarity.

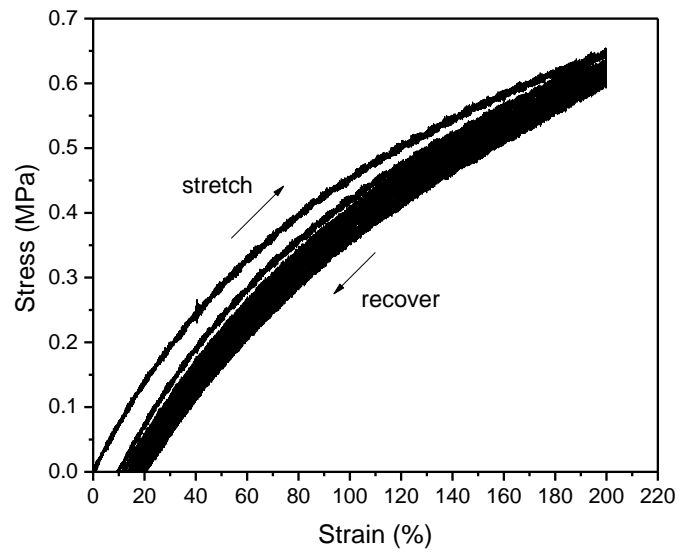


Fig. S41 Cyclic tensile test for TBPE-8 (200% stain, 10 mm min^{-1}).

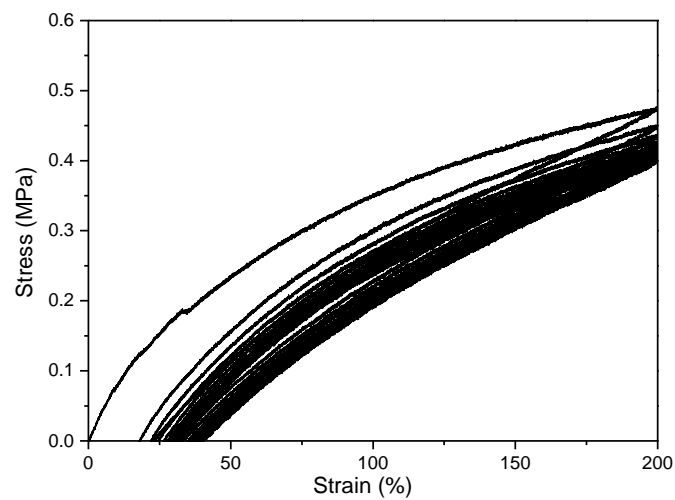


Fig. S42 Cyclic tensile tests for TBPE-9 (10 cycles 200 % strain, 10 mm min^{-1}).

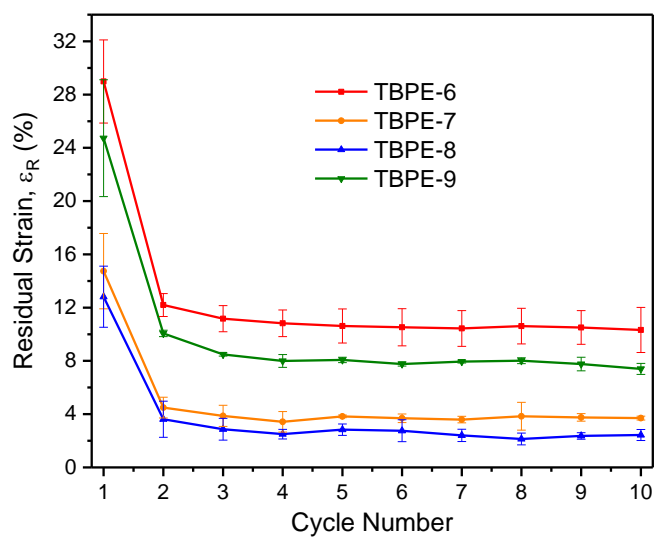
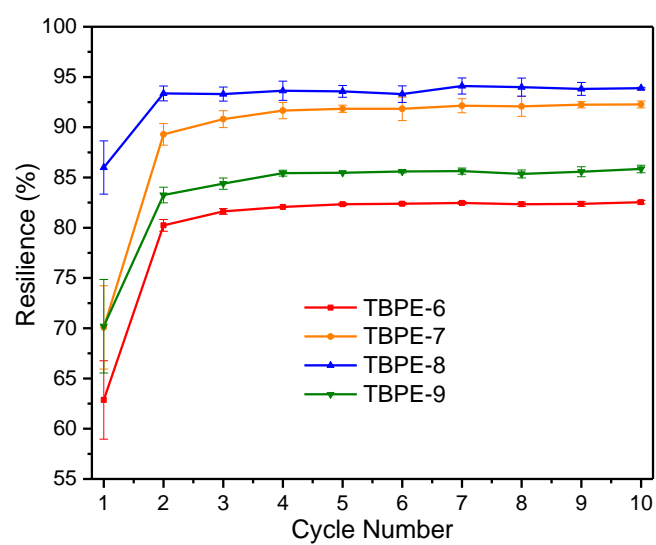


Figure S43. Cyclic tensile testing parameters as a function of cycle number for TBPEs-6 to -9; **Top:** Resilience and **Bottom:** Residual Strain. Samples were extended to a maximum of 200% strain at a rate of 10 mm min⁻¹. Error bars represent a standard deviation of 3 specimens.

Table S5. Elastic recovery (ER), resilience and residual strain (ϵ_R) of three dumbbell specimens of each of TBPE-6 to 9 after 10 hysteresis cycles to a maximum strain of 200%. s.d.= standard deviation. N.B. first cycle omitted from calculated mean and s.d.

Sample	ER (%) \pm s.d.	Resilience (%) \pm s.d.	ϵ_R (%) \pm s.d.
TBPE-5	94.3 \pm 0.2	74.1 \pm 2.1	11.5 \pm 0.3
	93.5 \pm 0.2	75.0 \pm 2.0	13.0 \pm 0.5
	92.3 \pm 0.3	73.6 \pm 2.1	15.5 \pm 0.7
Average	93.3 \pm 0.9	74.2 \pm 2.1	13.3 \pm 1.7
TBPE-6	94.1 \pm 0.2	81.9 \pm 0.8	11.8 \pm 0.5
	94.4 \pm 0.2	82.1 \pm 0.9	11.2 \pm 0.5
	95.3 \pm 0.4	82.2 \pm 0.5	9.4 \pm 0.8
Average	94.6 \pm 0.4	82.0 \pm 0.7	10.8 \pm 1.2
TBPE-7	98.3 \pm 0.3	92.4 \pm 0.5	3.4 \pm 0.6
	98.1 \pm 0.2	91.6 \pm 1.1	3.8 \pm 0.4
	97.9 \pm 0.3	90.9 \pm 1.2	4.2 \pm 0.6
Average	98.1 \pm 0.3	91.6 \pm 1.1	3.8 \pm 0.6
TBPE-8	98.6 \pm 0.3	94.3 \pm 0.5	2.6 \pm 0.7
	98.5 \pm 0.4	93.0 \pm 0.5	3.0 \pm 0.8
	98.9 \pm 0.2	93.8 \pm 0.5	2.2 \pm 0.4
Average	98.7 \pm 0.3	93.7 \pm 0.7	2.7 \pm 0.7
TBPE-9	95.1 \pm 0.4	85.3 \pm 0.7	8.2 \pm 0.7
	95.9 \pm 0.4	85.2 \pm 0.8	8.2 \pm 0.8
	95.9 \pm 0.4	85.0 \pm 0.4	8.1 \pm 0.9
Average	95.9 \pm 0.4	85.2 \pm 0.9	8.2 \pm 0.8

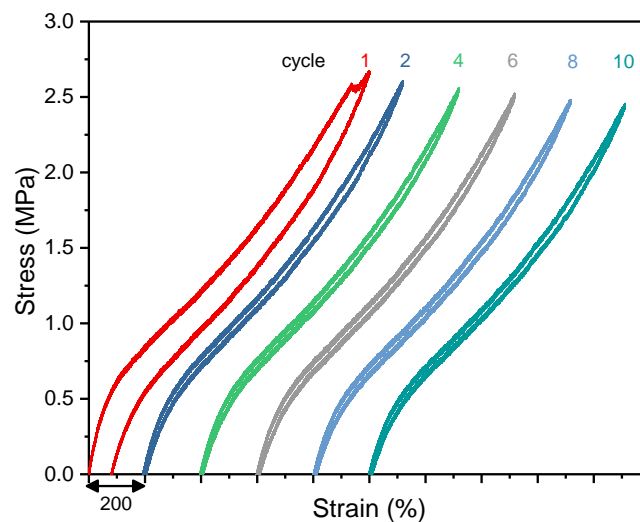


Fig. S44 Cyclic tensile test TBPE-8 to 1000% strain. Only alternate cycles, horizontally shifted are shown for clarity.

13. Order-to-Disorder Transition

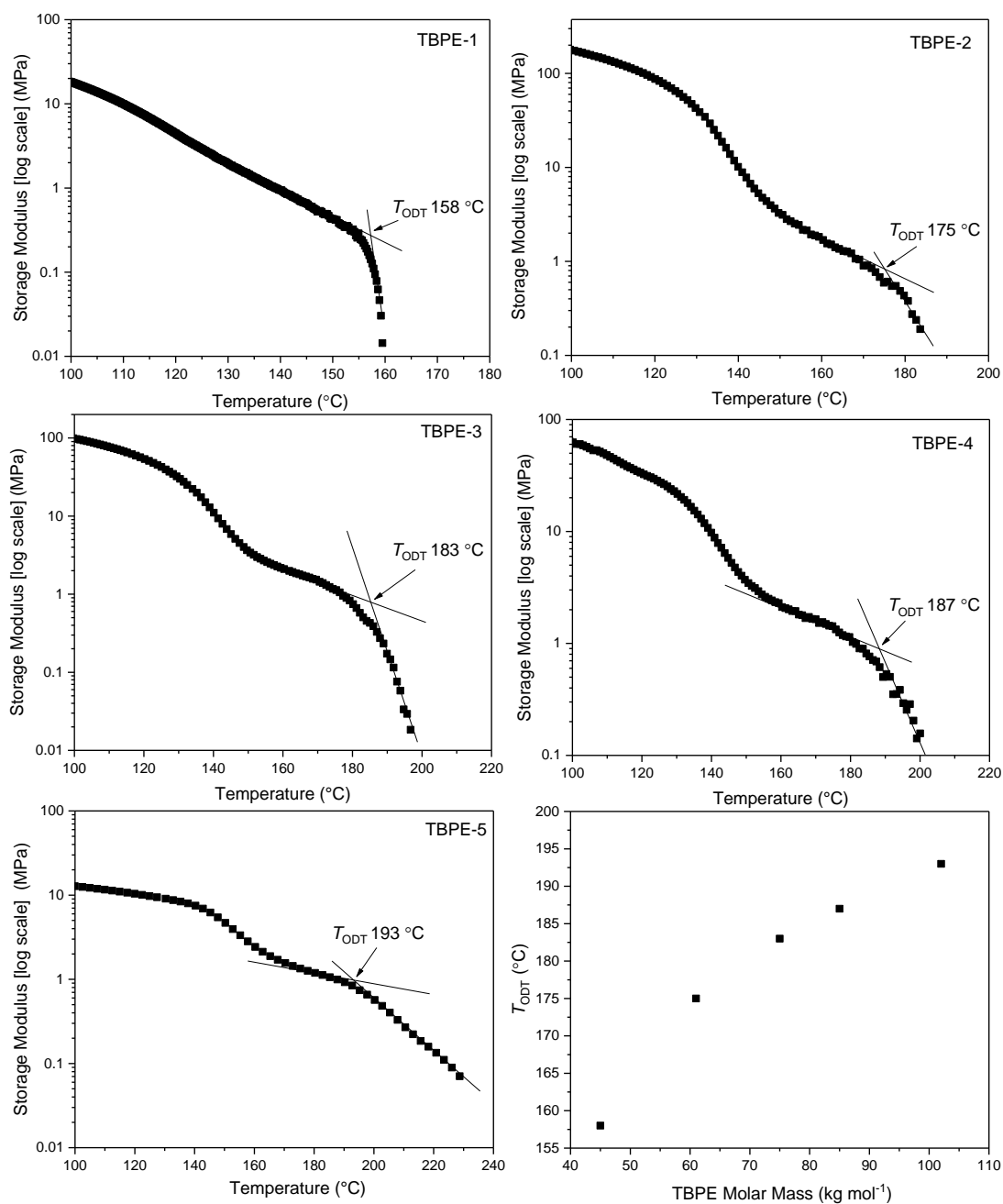


Fig. S45 Determination of order-to-disorder transition from storage modulus (G') as a function of temperature. The transition temperatures (T_{ODT}) were determined at the intersect of two extrapolated lines. Plot of measured T_{ODT} as a function of TBPE overall molar mass (determined by SEC-Table S1).

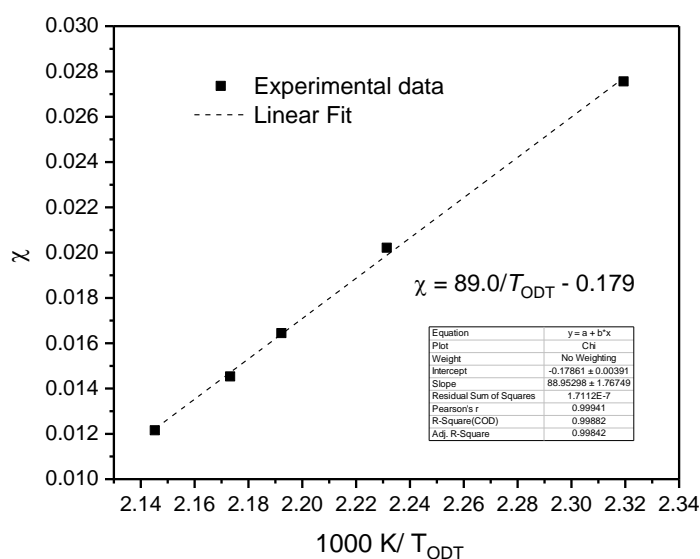


Fig. S46 Temperature dependence of χ . Order-to-disorder transition temperatures (T_{ODT}) were determined for TBPE-1 to 5 by DMA. N_{Total} was calculated from the total molar mass estimated by SEC and based on room temperature densities of PDL (0.97 g cm^{-3}) and P(PA-*alt*-CHO) (1.04 g cm^{-3}) and 118 \AA standard reference volume. $(\chi N)_{ODT}$ estimated based on phase diagram for monodisperse ABA triblock copolymers from Matsen.^[12]

Table S6. Comparison of χ with other literature values.

Triblock Copolymer	χ (150 °C)	Ref.
PE-PDL	0.035	This work
PLA-PDL	0.091	[6]
PLA-PM	0.36	[13]
PS-PLA	0.075	[14]
PLA-P6MCL	0.045	[15]
PLA-P γ MCL	0.052	[16]
PLA-PCD77	0.038	[17]
PLA-PCL	0.038	[17]
PS-PI	0.049	[18]

14. Thermal Gravimetric Analysis (TGA)

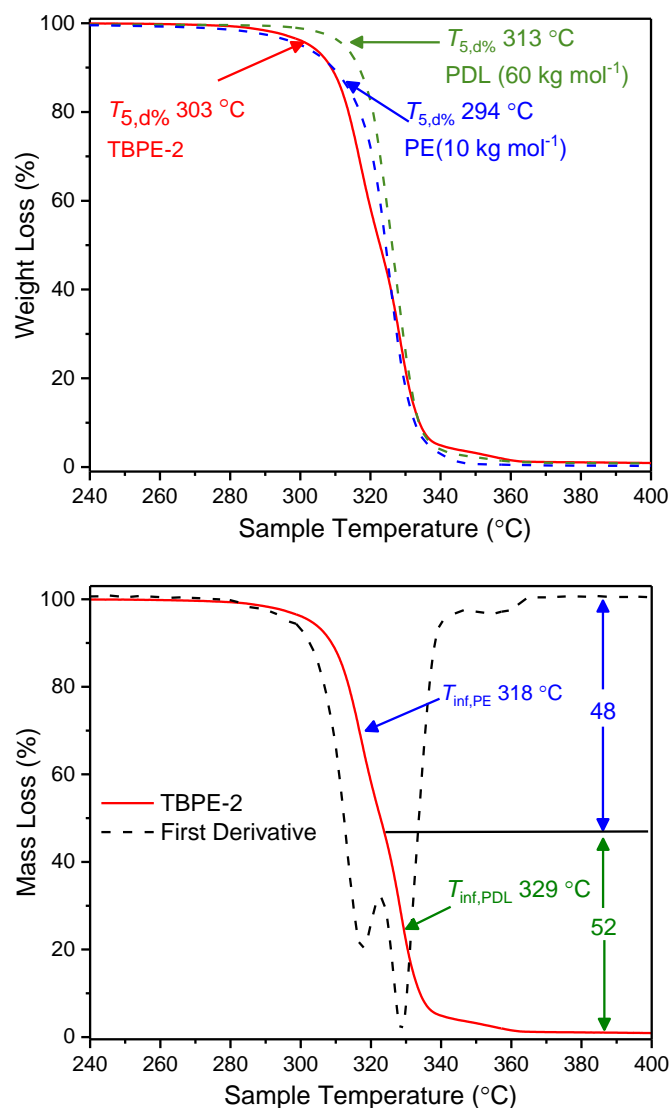


Fig. S47 TGA analysis. **Top:** TGA curve for TBPE-2 (25-500 °C, 5 °C min⁻¹, N₂ flow) compared to independent PDL and PE polymers. **Bottom:** TGA curve for TBPE-2 with first derivative showing two degradation steps assigned to the PE and PDL blocks.

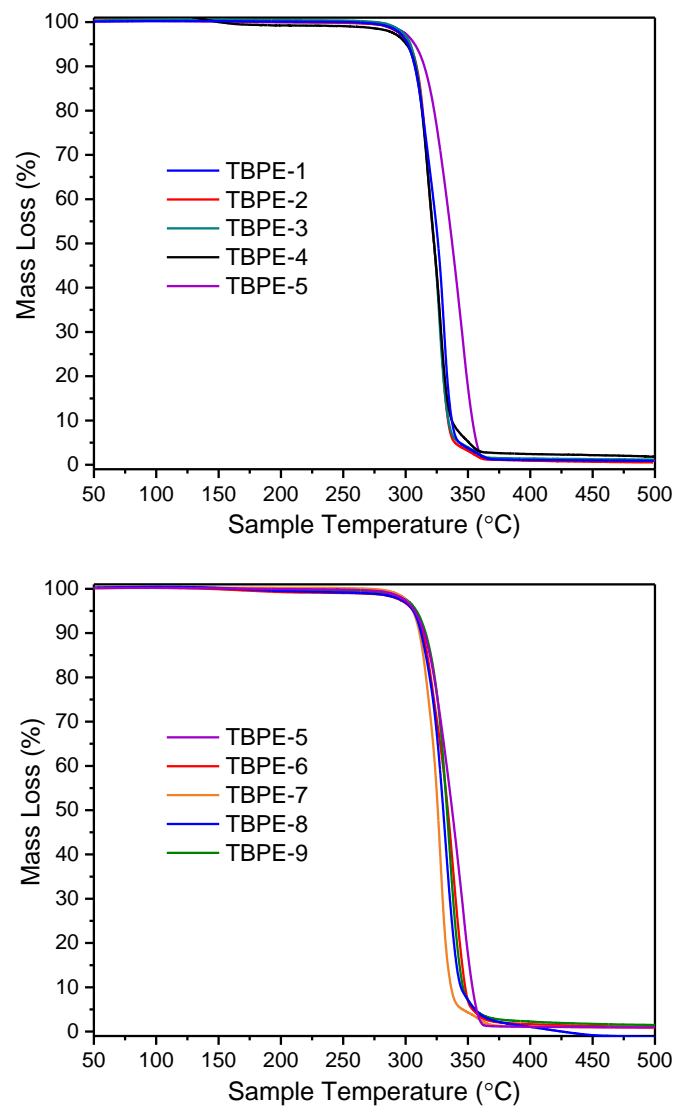


Fig. S48 TGA curves for TBPE-1 to -9 (**Top:** TBPE-1 to -5; **Bottom:** TBPE-5 to -9). The degradation behaviour of TBPE-5 is more in agreement with that observed for TBPE-6 to -9 and is attributed to similar overall molar mass ($M_n \sim 100 \text{ kg mol}^{-1}$), irrespective of block composition.

Table S7. TGA data for TBPE-1 to -9.^a

Sample	$T_{5\%,d}$ (°C) ^b	$T_{10\%,d}$ (°C) ^b	T_{end} (°C)	Total Mass loss (%)	$T_{inf 1}$ (°C) [% mass loss]	$T_{inf 2}$ (°C) [% mass loss]
PE(10.2 kg mol ⁻¹)	294	306	336	98.0	323	n.a.
PDL(60 kg mol ⁻¹)	313	317	335	99.4	328	n.a
TBPE-1	303	308	339	99.1	319 [35]	331[60]
TBPE-2	303	309	339	99.9	318 [48]	329 [52]
TBPE-3	304	309	338	98.8	317 [43]	327 [56]
TBPE-4	305	309	338	98.2	319 [48]	328 [50]
TBPE-5	307	315	355	99.3	331 [36]	345 [64]
TBPE-6	306	314	350	98.9	326 [31]	338 [68]
TBPE-7	307	312	367	99.2	319 [27]	328 [72]
TBPE-8	306	312	356	97.0	319 [19]	332 [78]
TBPE-9	309	316	355	98.5	n.d.	n.d.

^a 30 – 500 °C, N₂ flow, 5 °C min⁻¹ heating rate; ^b Temperature at which 5% mass lost; ^c Temperature after which 10% mass lost; ^d Final temperature after no further degradation observed (near complete mass loss); ^e Total % mass loss; ^f Inflection for first degradation step based on first derivative of TGA curve and corresponding mass loss from integration; ^g Inflection point of second degradation step and corresponding mass loss.

15. Small Angle X-ray Scattering (SAXS)

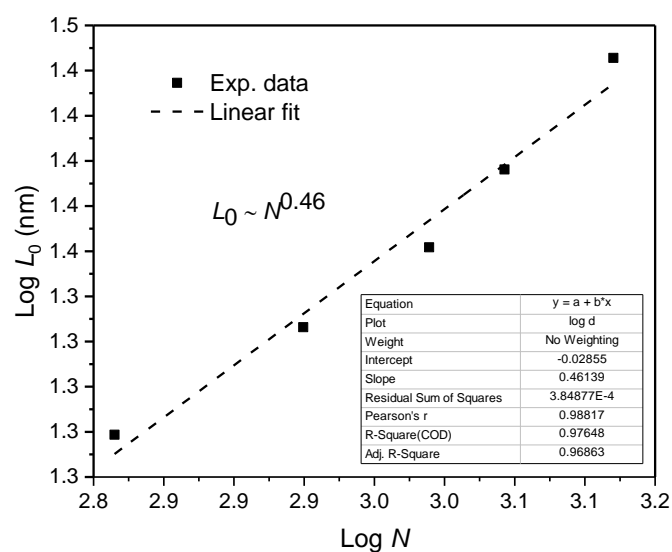


Fig. S49. Double logarithm plot of d versus N for TBPEs-1 to -5 of similar composition (f_{hard} 0.4-0.44). d Values are calculated from $d=2\pi/q^*$, where q^* is principal scattering peak at room temperature prior to annealing. Domain size roughly scales with N as $d \sim \chi^{1/6}N^\alpha$. Here calculated $\alpha \sim 0.5$ implies a weakly segregated system. This may be due to similar polarity of PDL and PE blocks.

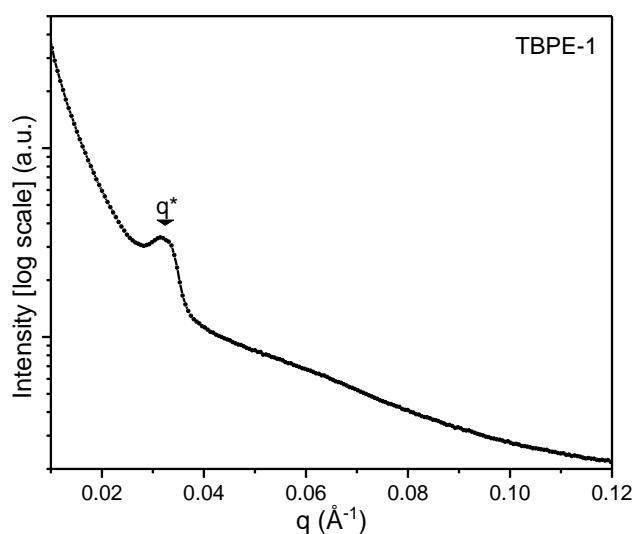


Fig. S50 SAXS pattern for TBPE-1 at room temperature.

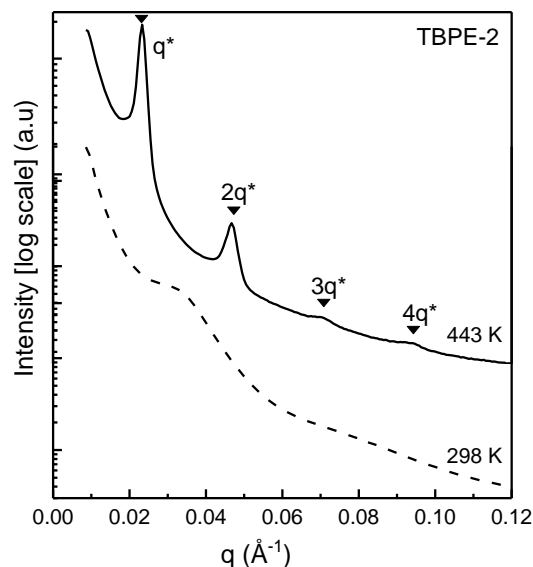


Fig. S51 TBPE-2 on heating revealing higher order peaks observed consistent with a lamellar morphology: q^* , $2q^*$, $3q^*$, $4q^*$.

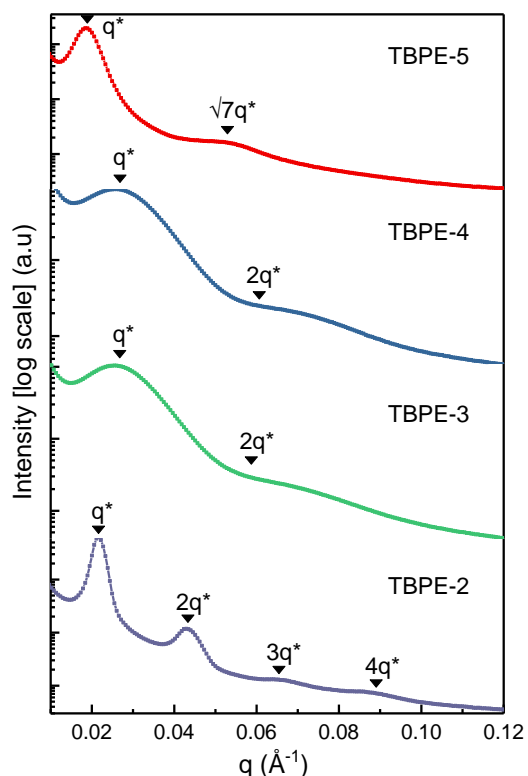


Fig. S52 TBPE-2,-3,-4,-5 recorded at room temperature after annealing at 200 °C. On heating a precipitated sample of TBPE-2 at 10 °C min⁻¹, higher order SAXS peaks were observed within a narrow temperature window (~175 °C) at q^* , $2q^*$, $3q^*$ and $4q^*$ consistent with a lamellar morphology. TBPE- 1 omitted for clarity (q^* at 0.03283 \AA^{-1} , $d = 19$ nm); (\blacktriangledown represents principal scattering peaks). For TBPE- 5, annealing led to sharper principal scattering peak and domain spacing of 34 nm.

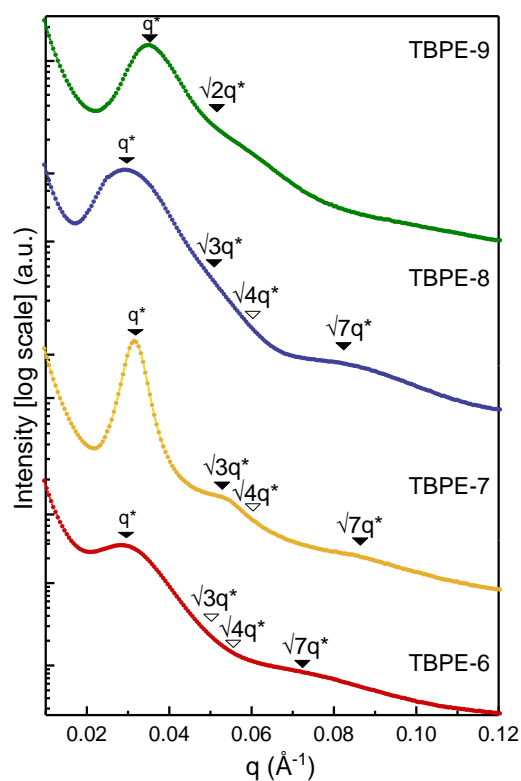


Fig. S53 SAXS data of elastomer series TBPE-6 to -9, recorded at room temperature, of polymer films which were subjected to annealing at 200 °C. TBPE-6,-7 and-8 are assigned to hexagonal pack cylinders (HEX) and TBPE-9 to spherical morphology. Observed values for allowed SAXS reflections (based on the principal scattering peak, q^*) are marked with \blacktriangledown and expected peaks not clearly observed/missing are identified with ∇ . Expected bragg maxima/allowed higher order SAXS reflections for microphase separated cylinders arranged on a hexagonal lattice: q^* , $\sqrt{3}q^*$, $\sqrt{4}q^*$, $\sqrt{7}q^*$, $\sqrt{9}q^*$, etc.; and spheres on a BCC lattice: q^* , $\sqrt{2}q^*$, $\sqrt{4}q^*$, $\sqrt{6}q^*$ etc.

16. Degradation Studies

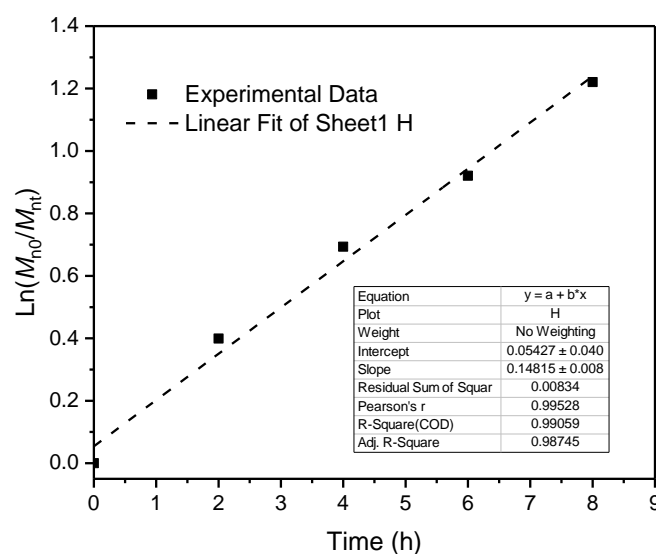


Fig. S54 Determination of initial degradation rate constant for degradation of TBPE-5 (toluene, *p*-TSA, 60 °C) based on first order kinetic model: $\text{Ln}(M_{nt}) = \text{Ln}(M_{n0}) - k_d t$, where M_n is the number average molar mass, determined here by SEC (vs PS standards) and M_{n0} , the molar mass prior to the start of hydrolysis. k_d = degradation rate constant and t = degradation time.^[19]

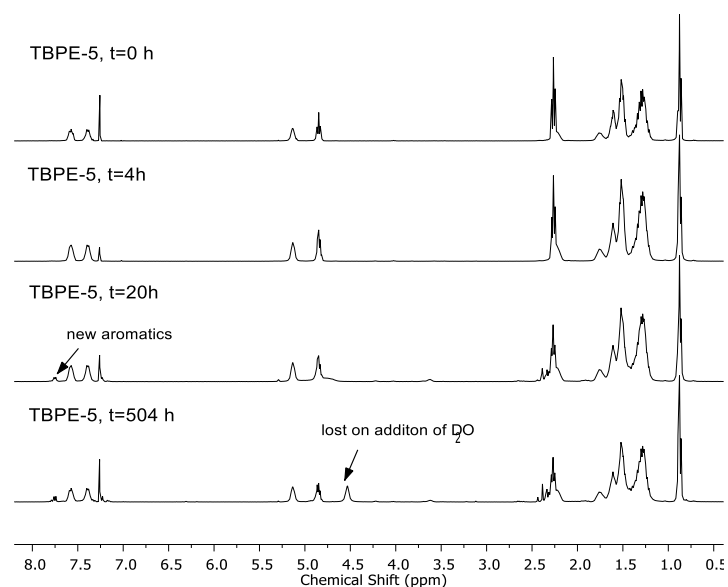


Fig. S55 ¹H NMR spectroscopic analysis of TBPE-5 degradation (*p*-TSA, toluene, 60 °C). After 4 h, the reaction spectrum is remarkably similar to the starting polymer film ($t = 0$ h) suggesting the formation of oligomers by chain scission reactions rather than hydrolysis to small molecules. After 20 h (M_n 20.4 kg mol⁻¹, \bar{D} 1.54), additional aromatic environments are observed. After 3 weeks (M_n 3.6 kg mol⁻¹, \bar{D} 2.19), the new resonance observed at 4.53 ppm is attributed to an -OH end-group and is lost on addition of D₂O.

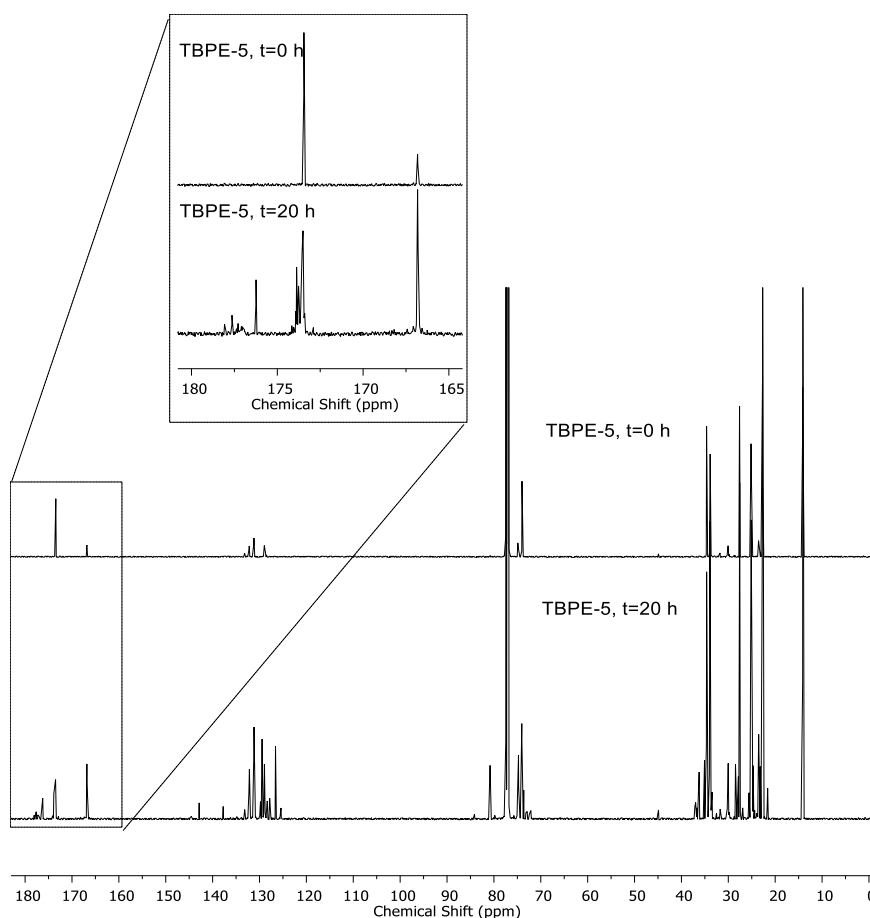


Fig. S56. $^{13}\text{C}\{^1\text{H}\}$ NMR spectra (CDCl_3) of TBPE-5 before degradation and after 20 h; inset carbonyl region showing evidence of formation of oligomers or transesterification.

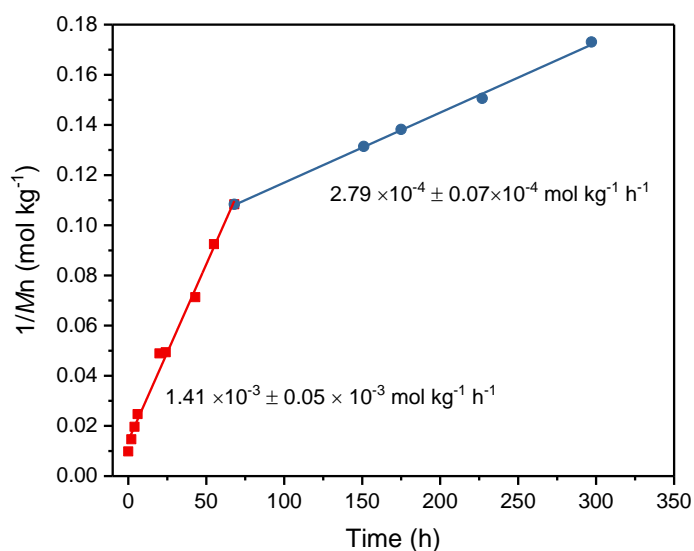


Fig. S57 Plot of $1/M_n$ versus time for degradation of TBPE-5 with $p\text{-TSA}\cdot\text{H}_2\text{O}$ in toluene at 60°C . $1/M_n$ is proportional to concentration of newly formed chains during polymer hydrolysis as described for example by Untereker and coworkers.^[20]

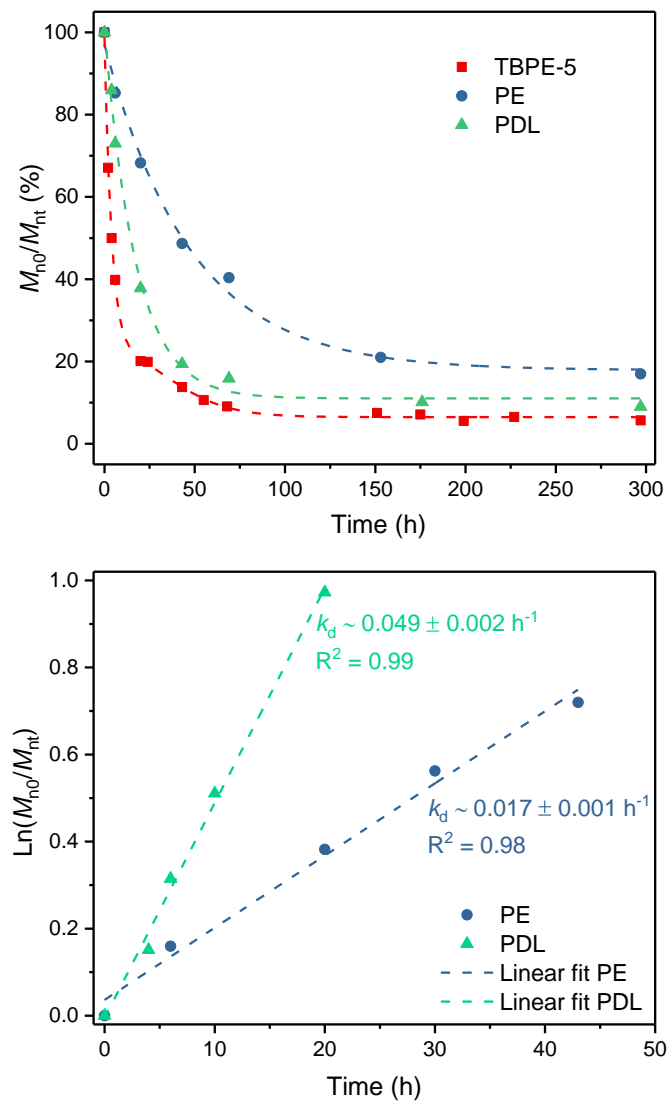


Fig. S58 Polyester degradation with *p*-TSA.H₂O in toluene at 60 °C. Comparison of TBPE-5 (102 kg mol⁻¹), PE (19.1 kg mol⁻¹) and PDL (60 kg mol⁻¹).

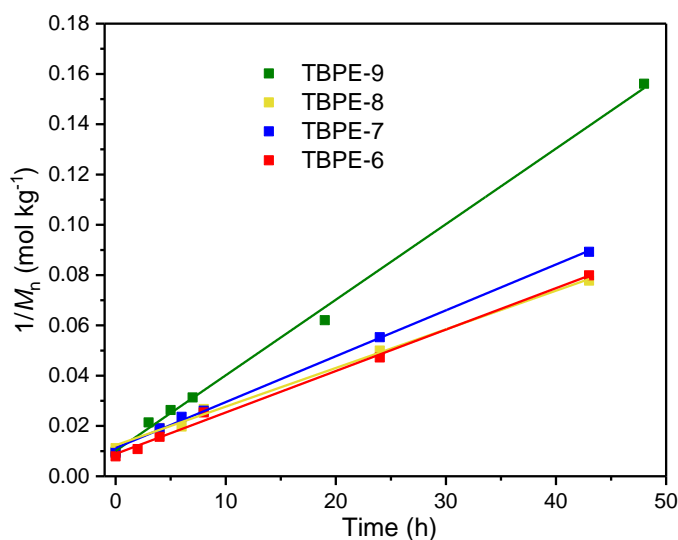


Fig. S59 Degradation of TBPE-6 to-9 with *p*-TSA (6 mM) in toluene (2 wt%). Plots of $1/M_n$ determined by SEC against time for aliquots taken at various time points.

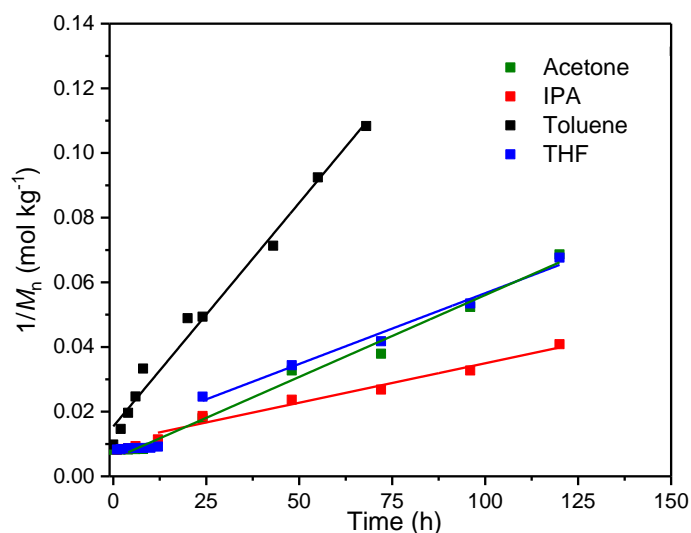


Fig. S60 Degradation of TBPE-5 in different solvents with *p*-TSA.H₂O at 60 °C.

Table S8. Static Water Contact Angles. Mean and standard deviation of 10 measurements for each sample.

Sample (f_{hard})	Water Contact Angle/°	Standard Deviation/°
TBPE-3 (0.40)	95.06	1.04
TBPE-5 (0.40)	75.53	2.38
TBPE-6 (0.29)	85.59	1.98
TBPE-7 (0.24)	96.57	1.77
TBPE-8 (0.19)	98.45	0.90
TBPE-9 (0.12)	98.02	1.65

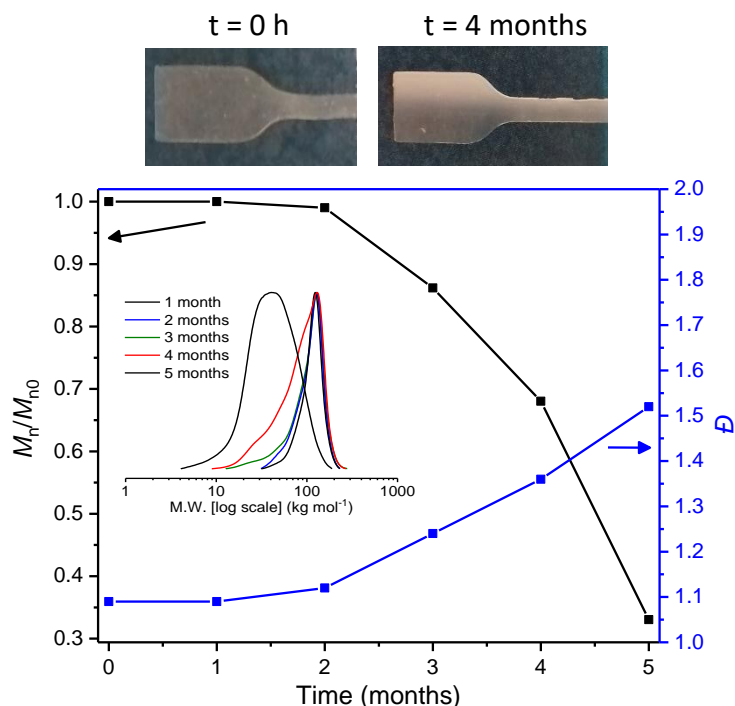


Fig. S61 Degradation of TBPE-5 in water (~2 wt%) with *p*-TSA (6 mM) at 60 °C. Top: visual changes observed in the polymer during the degradation experiment. Bottom: Change in molar mass determined by SEC normalised to original at $t = 0$ h (M_{n0}) and dispersity (\bar{D}); inset: SEC traces showing 67% molar mass loss from 102 to 34 kg mol⁻¹ after 5 months with concomitant increase in \bar{D} from 1.09 to 1.52.

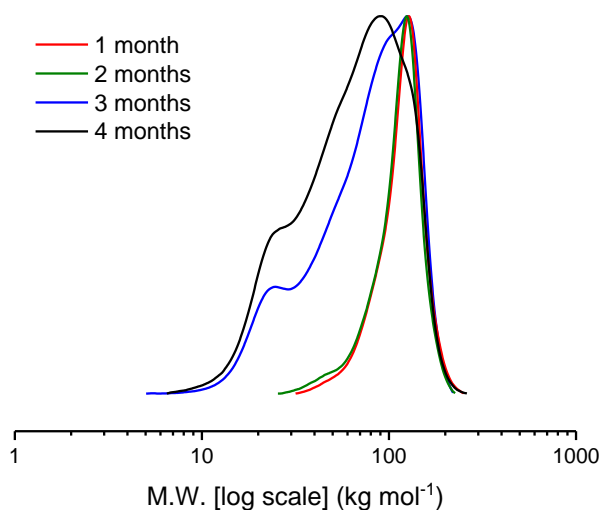


Fig. S62 SEC traces of aliquots taken during enzymatic degradation of TBPE-5 with Novozym[®] 51032 in PBS solution (pH 7.4) at 37 °C.

17. Comparison to Literature TPEs.

Table S9. Comparison of TBPE-6 to -9 (Table 2) literature and commercial TPEs examples.

Entry	Sample	M_n (kg mol ⁻¹)	f_{hard}	E_y (MPa)	ϵ_b (%)	σ_b (MPa)	Ref
1	MBPE-26	56.6	0.27	1.7 ± 0.6	2450 ± 450	12 ± 3	[5]
2	LDL	136	0.21	1.0 ± 0.1	1600 ± 200	4.5 ± 0.3	[6]
3	LDL	148	0.27	1.1 ± 0.1	1310 ± 40	9.4 ± 0.7	[6]
4	PLLA-PDL-PLLA	191	0.24	2.9 ± 0.3	1212 ± 25	13.6 ± 0.5	[9]
5	PLLA-PDL-PLLA	173	0.13	2.0 ± 0.2	1420 ± 59	4.23 ± 0.2	[9]
6	PLLA-PDL-PLLA	162	0.063	1.1 ± 0.1	323 ± 10	0.14 ± 0.1	[9]
4	PLA-γMCL-PLA	94	0.17	4.8 ± 0.2	1029 ± 20	24 ± 2	[16]
7	LCD69L	104	0.17	1.5 ± 0.3	2100 ± 100	9.9 ± 0.6	[17]

18. References

- [1] A. Spyros, D. S. Argyropoulos, R. H. Marchessault, *Macromolecules* **1997**, *30*, 327-329.
- [2] S. Kobayashi, H. Uyama, T. Takamoto, *Biomacromolecules* **2000**, *1*, 3-5.
- [3] J. Filik, A. W. Ashton, P. C. Y. Chang, P. A. Chater, S. J. Day, M. Drakopoulos, M. W. Gerring, M. L. Hart, O. V. Magdysyuk, S. Michalik, A. Smith, C. C. Tang, N. J. Terrill, M. T. Wharmby, H. Wilhelm, *J. Appl. Cryst.* **2017**, *50*, 959-966; B. R. Pauw, A. J. Smith, T. Snow, N. J. Terrill, A. F. Thunemann, *J. Appl. Cryst.* **2017**, *50*, 1800-1811.
- [4] G. S. Sulley, G. L. Gregory, T. T. D. Chen, L. P. Carrodeguas, G. Trott, A. Santmarti, K.-Y. Lee, N. J. Terrill, C. K. Williams, *Selective Catalysis Delivers Versatile Properties to CO₂-Derived Block Polymers*, *J. Am. Chem. Soc.* **2019**, under review.
- [5] Y. Zhu, M. R. Radlauer, D. K. Schneiderman, M. S. P. Shaffer, M. A. Hillmyer, C. K. Williams, *Macromolecules* **2018**, *51*, 2466-2475.
- [6] M. T. Martello, D. K. Schneiderman, M. A. Hillmyer, *ACS Sustain. Chem. Eng.* **2014**, *2*, 2519-2526.
- [7] S. Cheng, M. Rabnawaz, F. Khan, B. Khan, *J. Appl. Polym. Sci.* **2019**, *136*, 47200; X. Yu, J. Jia, S. Xu, K. U. Lao, M. J. Sanford, R. K. Ramakrishnan, S. I. Nazarenko, T. R. Hoyer, G. W. Coates, R. A. DiStasio, *Nat. Commun.* **2018**, *9*, 2880; H. Li, H. Luo, J. Zhao, G. Zhang, *Macromolecules* **2018**, *51*, 2247-2257; K. Bester, A. Bukowska, B. Myśliwiec, K. Hus, D. Tomczyk, P. Urbaniak, W. Bukowski, *Polym. Chem.* **2018**, *9*, 2147-2156; G. Si, L. Zhang, B. Han, Z. Duan, B. Li, J. Dong, X. Li, B. Liu, *Polym. Chem.* **2015**, *6*, 6372-6377; P. K. Saini, C. Romain, Y. Zhu, C. K. Williams, *Polym. Chem.* **2014**, *5*, 6068-6075; L. Lin, J. Liang, Y. Xu, S. Wang, M. Xiao, L. Sun, Y. Meng, *Green Chem.* **2019**, *21*, 2469-2477; S. Cheng, B. Khan, F. Khan, M. Rabnawaz, *Polymers* **2018**, *10*.
- [8] A. X. H. Yong, G. D. Sims, S. J. P. Gnaniah, S. L. Ogin, P. A. Smith, *Advanced Manufacturing: Polymer & Composites Science* **2017**, *3*, 43-51.
- [9] S. Lee, K. Lee, Y.-W. Kim, J. Shin, *ACS Sustain. Chem. Eng.* **2015**, *3*, 2309-2320.
- [10] E. Guth, *J. Appl. Phys.* **1945**, *16*, 20-25.
- [11] Z. Wang, L. Yuan, F. Jiang, Y. Zhang, Z. Wang, C. Tang, *ACS Macro Lett.* **2016**, *5*, 220-223.
- [12] M. W. Matsen, *J. Chem. Phys.* **2000**, *113*, 5539-5544.
- [13] M. A. Hillmyer, W. B. Tolman, *Acc. Chem. Res.* **2014**, *47*, 2390-2396.
- [14] A. S. Zalusky, R. Olayo-Valles, J. H. Wolf, M. A. Hillmyer, *J. Am. Chem. Soc.* **2002**, *124*, 12761-12773.
- [15] M. T. Martello, M. A. Hillmyer, *Macromolecules* **2011**, *44*, 8537-8545.
- [16] A. Watts, N. Kurokawa, M. A. Hillmyer, *Biomacromolecules* **2017**, *18*, 1845-1854.
- [17] D. K. Schneiderman, E. M. Hill, M. T. Martello, M. A. Hillmyer, *Polym. Chem.* **2015**, *6*, 3641-3651.
- [18] C. C. Lin, S. V. Jonnalagadda, P. K. Kesani, H. J. Dai, N. P. Balsara, *Macromolecules* **1994**, *27*, 7769-7780.
- [19] V. Karmore, G. Madras, *Ind. Eng. Chem. Res.* **2001**, *40*, 1306-1311.
- [20] Lyu, J. Schley, B. Loy, D. Lind, C. Hobot, R. Sparer, D. Untereker, *Biomacromolecules* **2007**, *8*, 2301-2310.